

**Supporting Information**  
for  
**Nitric Oxide Reactivity of Copper(II) Complexes of Bidentate Amine Ligands: Effect of  
Substitution on Ligand Nitrosation**

Moushumi Sarma and Biplab Mondal\*

*Department of Chemistry, Indian Institute of Technology Guwahati, Assam – 781039, India.*

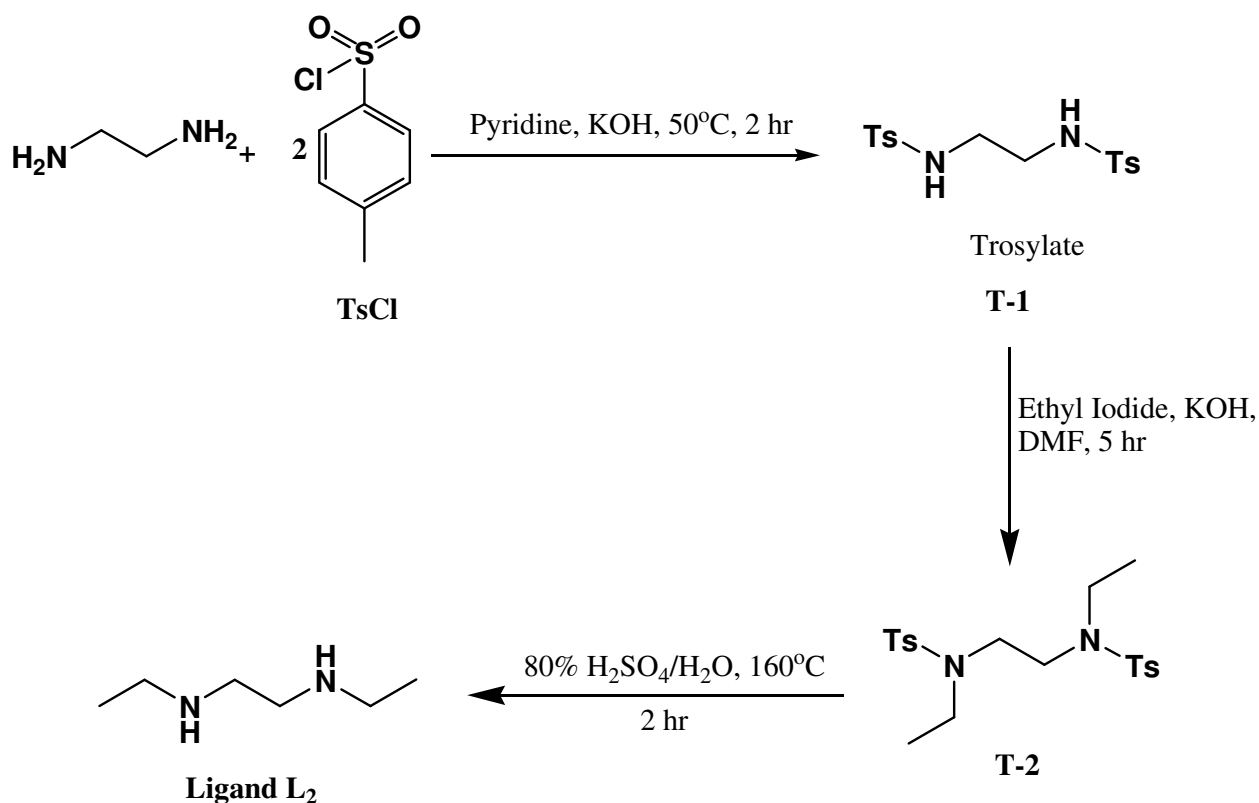
<b>Table of Contents</b>	<b>Page</b>
Synthesis of ligand L <sub>2</sub> and L <sub>3</sub> .	03
<b>Figure S1:</b> FT-IR spectrum of <b>T-1</b> in KBr pellet.	06
<b>Figure S2:</b> <sup>1</sup> H NMR spectrum of <b>T-1</b> in CDCl <sub>3</sub> .	06
<b>Figure S3:</b> <sup>13</sup> C NMR spectrum of <b>T-1</b> in CDCl <sub>3</sub> .	07
<b>Figure S4:</b> ESI-Mass spectrum of <b>T-1</b> in methanol.	07
<b>Figure S5:</b> FT-IR spectrum of <b>T-2</b> in KBr pellet.	08
<b>Figure S6:</b> <sup>1</sup> H NMR spectrum of <b>T-2</b> in CDCl <sub>3</sub> .	08
<b>Figure S7:</b> <sup>13</sup> C NMR spectrum of <b>T-2</b> in CDCl <sub>3</sub> .	09
<b>Figure S8:</b> ESI-Mass spectrum of <b>T-2</b> in methanol.	09
<b>Figure S9:</b> FT-IR spectrum of <b>L<sub>2</sub></b> in KBr pellet.	10
<b>Figure S10:</b> <sup>1</sup> H NMR spectrum of <b>L<sub>2</sub></b> in CDCl <sub>3</sub> .	10
<b>Figure S11:</b> <sup>13</sup> C NMR spectrum of <b>L<sub>2</sub></b> in CDCl <sub>3</sub> .	11
<b>Figure S12:</b> ESI-Mass spectrum of <b>L<sub>2</sub></b> in methanol.	11
<b>Figure S13:</b> FT-IR spectrum of <b>T-3</b> in KBr pellet.	12
<b>Figure S14:</b> <sup>1</sup> H NMR spectrum of <b>T-3</b> in CDCl <sub>3</sub> .	12
<b>Figure S15:</b> <sup>13</sup> C NMR spectrum of <b>T-3</b> in CDCl <sub>3</sub> .	13
<b>Figure S16:</b> ORTEP of <b>T-3</b> .	13
<b>Figure S17:</b> FT-IR spectrum of <b>L<sub>3</sub></b> in KBr pellet.	14
<b>Figure S18:</b> <sup>1</sup> H NMR spectrum of <b>L<sub>3</sub></b> in CDCl <sub>3</sub> .	14
<b>Figure S19:</b> <sup>13</sup> C NMR spectrum of <b>L<sub>3</sub></b> in CDCl <sub>3</sub> .	15
<b>Figure S20:</b> ESI-Mass spectrum of <b>L<sub>3</sub></b> in methanol.	15
<b>Figure S21:</b> FT-IR spectrum of complex <b>1</b> in KBr pellet.	16
<b>Figure S22:</b> FT-IR spectrum of complex <b>2</b> in KBr pellet.	16
<b>Figure S23:</b> FT-IR spectrum of complex <b>3</b> in KBr pellet.	17
<b>Figure S24:</b> X-Band EPR of complex <b>1</b> in acetonitrile at 77K.	17
<b>Figure S25:</b> X-Band EPR of complex <b>2</b> in acetonitrile at 77K.	18
<b>Figure S26:</b> X-Band EPR of complex <b>3</b> in acetonitrile at 77K.	18
<b>Figure S27:</b> Cyclic voltammogram of complex <b>1</b> in acetonitrile.	19
<b>Figure S28:</b> Cyclic voltammogram of complex <b>2</b> in acetonitrile.	19
<b>Figure S29:</b> Cyclic voltammogram of complex <b>3</b> in acetonitrile.	20
<b>Figure S30:</b> UV-visible spectra of the reaction of complex <b>1</b> with nitric oxide in acetonitrile.	20

<b>Figure S31:</b> UV-visible spectra of the reaction of complex <b>2</b> with nitric oxide in acetonitrile.	21
<b>Figure S32:</b> X-Band EPR spectra of complex <b>1</b> before and after purging NO at room temperature.	21
<b>Figure S33:</b> X-Band EPR spectra of complex <b>2</b> before and after purging NO at room temperature.	22
<b>Figure S34:</b> Solution IR spectra complex <b>2</b> in acetonitrile.	22
<b>Figure S35:</b> Solution IR spectra complex <b>3</b> in acetonitrile.	23
<b>Figure S36:</b> FT-IR spectrum of $L_1'$ in KBr pellet.	23
<b>Figure S37:</b> $^1H$ NMR $L_1'$ of in $CDCl_3$ .	24
<b>Figure S38:</b> $^{13}C$ NMR $L_1'$ of in $CDCl_3$ .	24
<b>Figure S39:</b> ESI-mass spectrum of $L_1'$ in methanol.	25
<b>Figure S40:</b> FT-IR spectrum of $L_1''$ in KBr pellet.	25
<b>Figure S41:</b> $^1H$ NMR $L_1''$ of in $CDCl_3$ .	26
<b>Figure S42:</b> $^{13}C$ NMR $L_1''$ of in $CDCl_3$ .	26
<b>Figure S43:</b> FT-IR spectrum of $L_2'$ in KBr pellet.	27
<b>Figure S44:</b> $^1H$ NMR $L_2'$ of in $CDCl_3$ .	27
<b>Figure S45:</b> $^{13}C$ NMR $L_2'$ of in $CDCl_3$ .	28
<b>Figure S46:</b> ESI-mass spectrum of $L_2'$ in methanol.	28
<b>Figure S47:</b> FT-IR spectrum of $L_2''$ in KBr pellet.	29
<b>Figure S48:</b> $^1H$ NMR $L_2''$ of in $CDCl_3$ .	29
<b>Figure S49:</b> $^{13}C$ NMR $L_2''$ of in $CDCl_3$ .	30
<b>Figure S50:</b> ESI-Mass spectrum of $L_2''$ in methanol.	30
<b>Figure S51:</b> FT-IR spectrum of $L_3'$ in KBr pellet.	31
<b>Figure S52:</b> $^1H$ NMR $L_3'$ of in $CDCl_3$ .	31
<b>Figure S53:</b> $^{13}C$ NMR $L_3'$ of in $CDCl_3$ .	32
<b>Figure S54:</b> ESI-Mass spectrum of $L_3'$ in methanol.	32
<b>Figure S55:</b> FT-IR spectrum of $L_3''$ in KBr pellet.	33
<b>Figure S56:</b> $^1H$ NMR $L_3''$ of in $CDCl_3$ .	33
<b>Figure S57:</b> $^{13}C$ NMR $L_3''$ of in $CDCl_3$ .	34
<b>Figure S58:</b> ESI-Mass spectrum of $L_3''$ in methanol.	34
<b>Table S1:</b> Crystallographic Data for ligand $L_1''$ .	35
<b>Table S3:</b> selected bond lengths and bond angles for ligand $L_1''$ .	35
<b>Table S3:</b> Crystallographic Data for ligand <b>T-3</b> .	36
Synthesis of copper(II) complex with tetramethylethylenediamine, <b>Complex 4</b>	37
<b>Figure S59:</b> UV-visible spectrum of Copper(II) complex of TMEDA ligand ( <b>Complex 4</b> ) in acetonitrile.	37
<b>Figure S60:</b> X-band EPR spectrum of complex <b>4</b> in acetonitrile at room temperature.	38
<b>Figure S61:</b> FT-IR spectrum of complex <b>4</b> in KBr.	38
<b>Figure S62:</b> UV-visible spectra of the reaction of complex <b>4</b> with nitric oxide in acetonitrile solvent at room temperature.	39
<b>Figure S63:</b> Solution FT-IR spectra complex <b>4</b> in acetonitrile.	39
<b>Figure S64:</b> X-Band EPR spectra of complex <b>4</b> before (blue trace) and after (red trace) purging NO in acetonitrile at room temperature.	40

### Synthesis of ligands L<sub>2</sub> and L<sub>3</sub>:

The ligands L<sub>2</sub> and L<sub>3</sub> were synthesized using a same experimental protocol. The details were given for L<sub>2</sub>.

Ligand L<sub>2</sub> was synthesized in three steps (scheme S1):



### Scheme S1

#### Step I. Tosylation of ethylenediamine:

A 250-ml two-necked round-bottomed flask equipped with a magnetic stirring bar, reflux condenser and a rubber septum was charged with ethylenediamine (0.360 g; 6 mmol), pyridine (20 ml) and potassium hydroxide (1.01 g; 18 mmol). The mixture was stirred and cooled in an

ice bath while 3.43 g (18 mmol) of tosyl chloride was added over a period of 5 min. After 5 min, the ice bath was removed and the reaction mixture was heated to 50 °C in an oil bath for 2 h with constant stirring. The reaction mixture was allowed to cool to room temperature was then poured into 20 ml ice-cold water. The crude tosylated product was obtained as whitish precipitate. The precipitate was purified by column chromatography using hexane to give 1.9 g (~ 85%) of N, N'-*p*-methylbenzenesulfonamide ethylenediamine(**T-1**). FT-IR: 1408, 1335, 1158 cm<sup>-1</sup>. <sup>1</sup>H-NMR (400 MHz, CDCl<sub>3</sub>): δ<sub>ppm</sub> 7.69(d, 4H, *J* = 8 Hz) 7.28(d, 4H, *J* = 8 Hz), 3.02(t, 4H, *J* = 8 Hz), 2.40(s, 6H). <sup>13</sup>C-NMR (100 MHz, CDCl<sub>3</sub>): δ<sub>ppm</sub>, 140.09, 137.58, 127.63, 125.67, 49.01, 21.80. (m+1)/z: 369.21.

### Step II: Ethylation of T-1:

A 250-ml two-necked round-bottomed flask equipped with a magnetic stirring bar, reflux condenser and a rubber septum was charged with 1.1 g ( 3 mmol) of **T-1**, 1.1 g (21 mmol) of potassium hydroxide, and 20 ml of anhydrous dimethylformamide (DMF). To this 2 g (12 mmol) ethyl iodide was added over a period of 5 min and the resulting mixture was heated at 60 °C in an oil bath for 4h. The reaction mixture was then allowed to cool to room temperature, diluted with 250 ml of water, and extracted with CHCl<sub>3</sub> (100 ml x 3 portions). The combined organic extracts were washed with brine (100 ml), dried over anhydrous sodium sulphate and concentrated under reduced pressure to give pale yellow oil. The oil was purified by column chromatography on neutral alumina to give 0.85 g (~65%) of **T-2** as a viscous pale yellow liquid FT-IR: 1408, 1335, 1158 cm<sup>-1</sup>. <sup>1</sup>H-NMR (400 MHz, CDCl<sub>3</sub>): δ<sub>ppm</sub> 7.66(d, 4H, *J* = 8 Hz) 7.29(d, 4H, *J* = 8 Hz), 3.25(s, 4H). 3.20(q, 4H, *J* = 8 Hz), 2.40(s, 6H), 1.143(s, 6H). <sup>13</sup>C-NMR (100 MHz, CDCl<sub>3</sub>): δ<sub>ppm</sub>, 143.62, 136.34, 129.96, 127.32, 48.21, 44.76, 21.69, 14.31. (m+1)/z: 425.71.

### Step III. Hydrolysis of T-2:

A 100-ml two-necked round-bottomed flask equipped with a magnetic stirring bar, reflux condenser, and a rubber septum was charged with 4.24 (10 mmol) of **T-2**, 17 ml of 80% H<sub>2</sub>SO<sub>4</sub>, and the resulting mixture was heated at 160 °C in an oil bath with constant stirring till solid goes

into solution. The reaction mixture was then allowed to cool to room temperature, diluted with 30 ml of water and neutralized with 20% NaOH solution. The resulting amine was then extracted with 3 x 50 ml portions of dichloromethane. The combined organic extracts were washed with brine (100 ml), dried over anhydrous sodium sulphate and concentrated under reduced pressure. The residue was purified by column chromatography on neutral alumina to give 0.75 g (~65%) of the desired amine **L<sub>2</sub>**. FT-IR: 1561, 1484, 1307, 1121, 719 $\text{cm}^{-1}$ . <sup>1</sup>H-NMR (400 MHz, CDCl<sub>3</sub>):  $\delta_{\text{ppm}}$ : 2.70 (s, 4H), 2.63 (q, 4H,  $J = 8$  Hz), 1.60(s, 1H), 1.08(t, 6H,  $J = 8$  Hz). <sup>13</sup>C-NMR (100 MHz, CDCl<sub>3</sub>):  $\delta_{\text{ppm}}$  49.26, 44.23, 15.30; (m+1)/z: 117.21.

### Synthesis of ligand **L<sub>3</sub>**:

#### Isobutylation of **T-1**:

Yield: 2.65g (72%) of **T-3** as a colorless crystalline solid. Its structure was also determined by the X-ray single structure. FT-IR: 1344, 1157, 1005, 725, 654  $\text{cm}^{-1}$ . <sup>1</sup>H-NMR (400 MHz, CDCl<sub>3</sub>):  $\delta_{\text{ppm}}$ . 7.65(d, 4H,  $J = 8.0$  Hz) 7.30(d, 4H,  $J = 8.0$  Hz), 3.18(s, 4H). 2.83(d, 4H,  $J = 8.0$  Hz), 2.41(s, 6H), 1.86(m, 2H) 0.917d, 6H,  $J = 8.0$  Hz).  $\delta_{\text{ppm}}$ , 143.67, 135.71, 129.93, 127.45, 58.24, 49.38, 27.45, 20.191.

#### Hydrolysis of **T-3**:

Yield: 0.56 g (32%) of the desired amine **L<sub>3</sub>**. FT-IR: 2957, 2923, 2853, 1465, 1089 $\text{cm}^{-1}$ . <sup>1</sup>H-NMR (400 MHz, CDCl<sub>3</sub>):  $\delta_{\text{ppm}}$ . 2.65 (s, 4H), 2.37 (d, 4H,  $J = 8.0$  Hz), 1.69(m, 2H), 0.85(d, 12H,  $J = 8.0$  Hz). <sup>13</sup>C-NMR (100 MHz, CDCl<sub>3</sub>):  $\delta_{\text{ppm}}$  58.08, 49.47, 28.42, 20.80; (m+1)/z: 173.21.

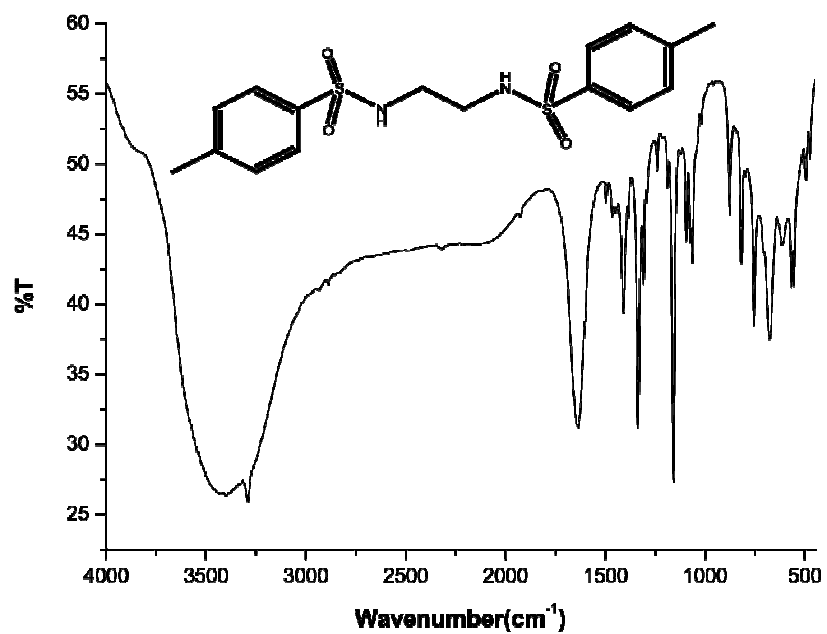


**Figure S1:** FT-IR spectrum of T-1 in KBr pellet.

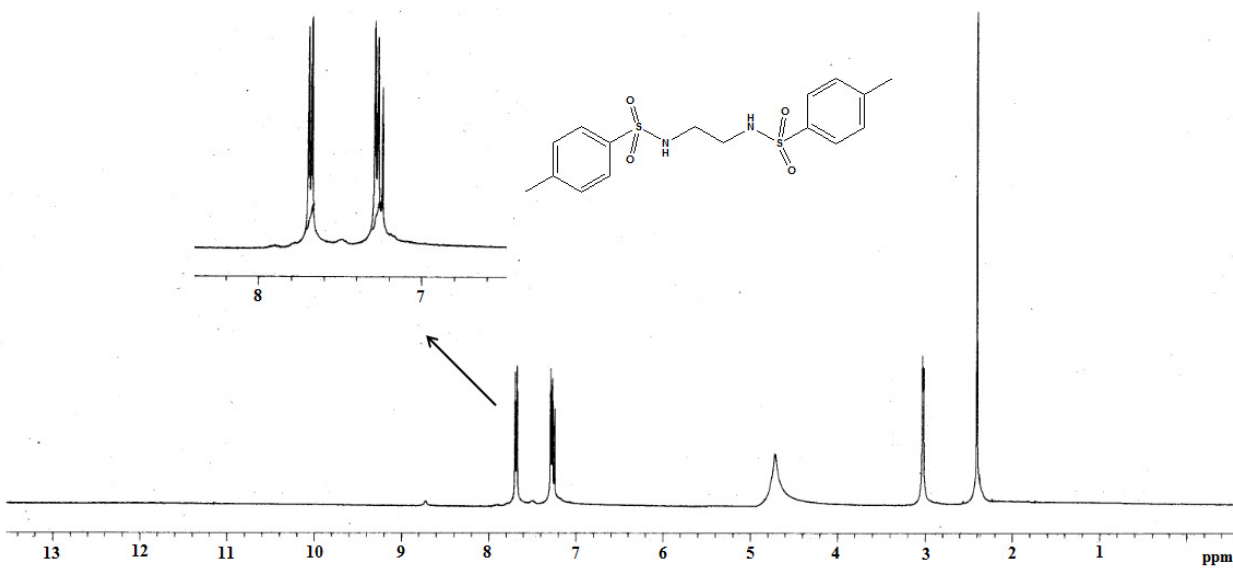


**Figure S2:** <sup>1</sup>H-NMR spectrum of T-1 in CDCl<sub>3</sub>.

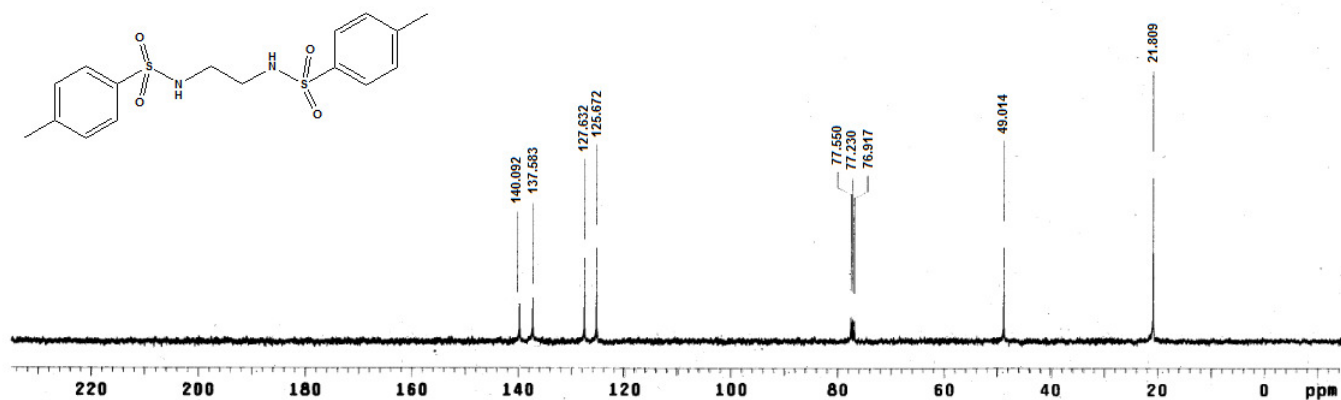


Figure S3:  $^{13}\text{C}$ -NMR spectrum of **T-1** in  $\text{CDCl}_3$ .

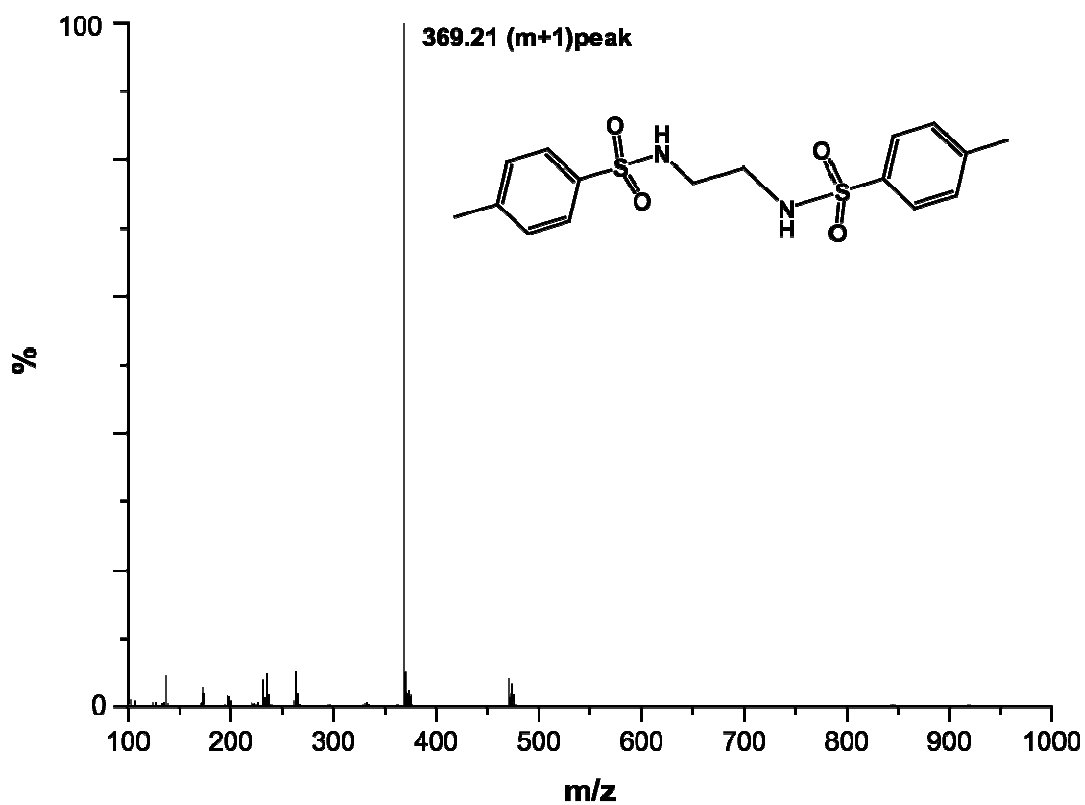
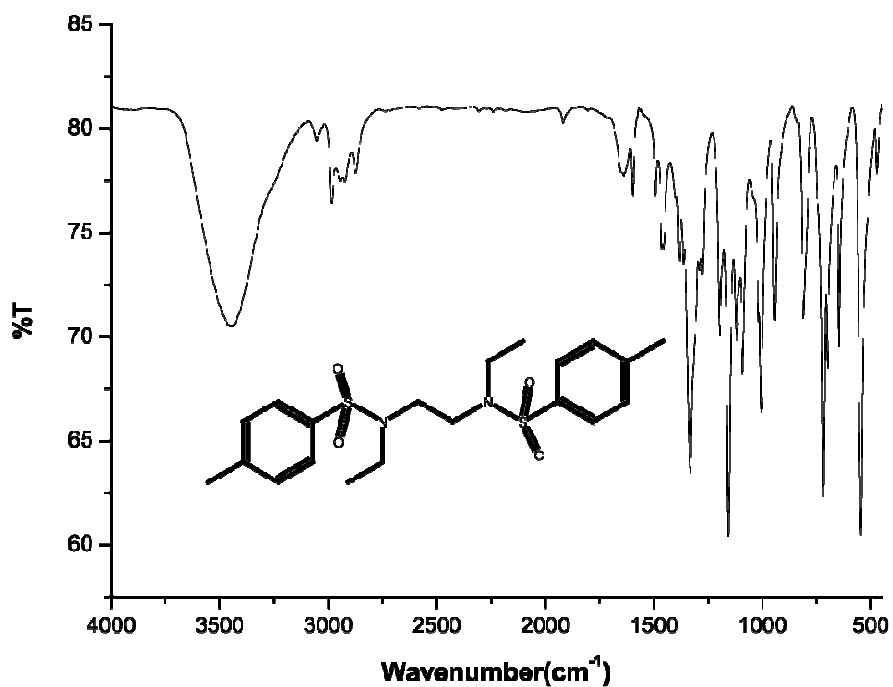
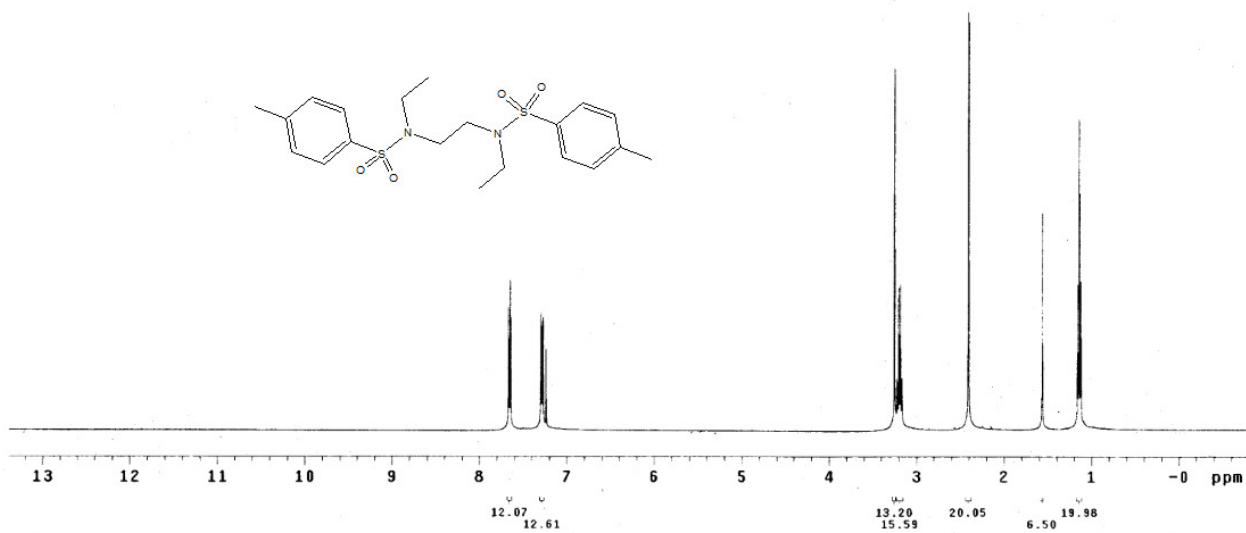


Figure S4: ESI-Mass spectrum of **T-1** in methanol.



**Figure S5:** FT-IR spectrum of T-2 in KBr pellet.



**Figure S6:** <sup>1</sup>H-NMR spectrum of T-2 in CDCl<sub>3</sub>.

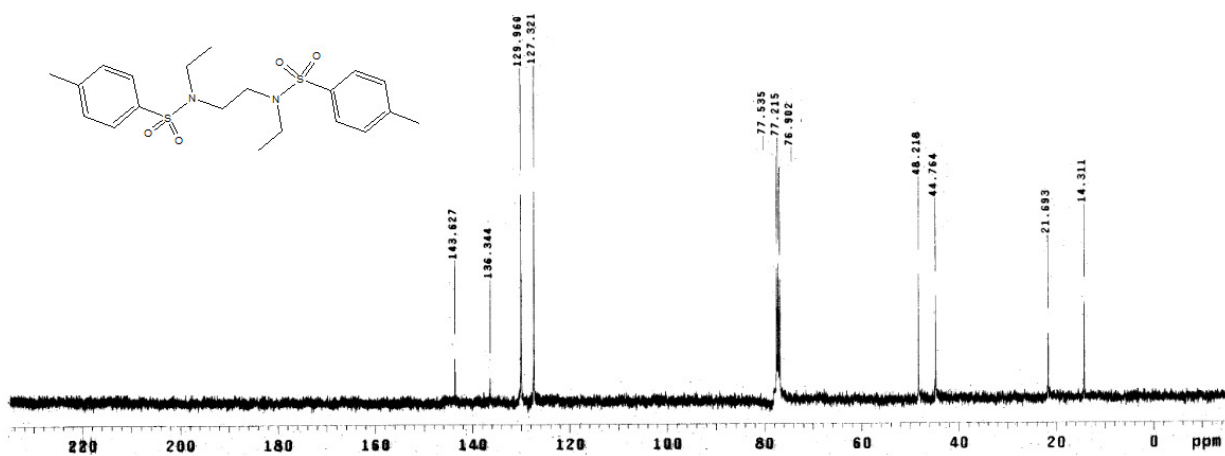


Figure S7:  $^{13}\text{C}$ -NMR spectrum of T-2 in  $\text{CDCl}_3$ .

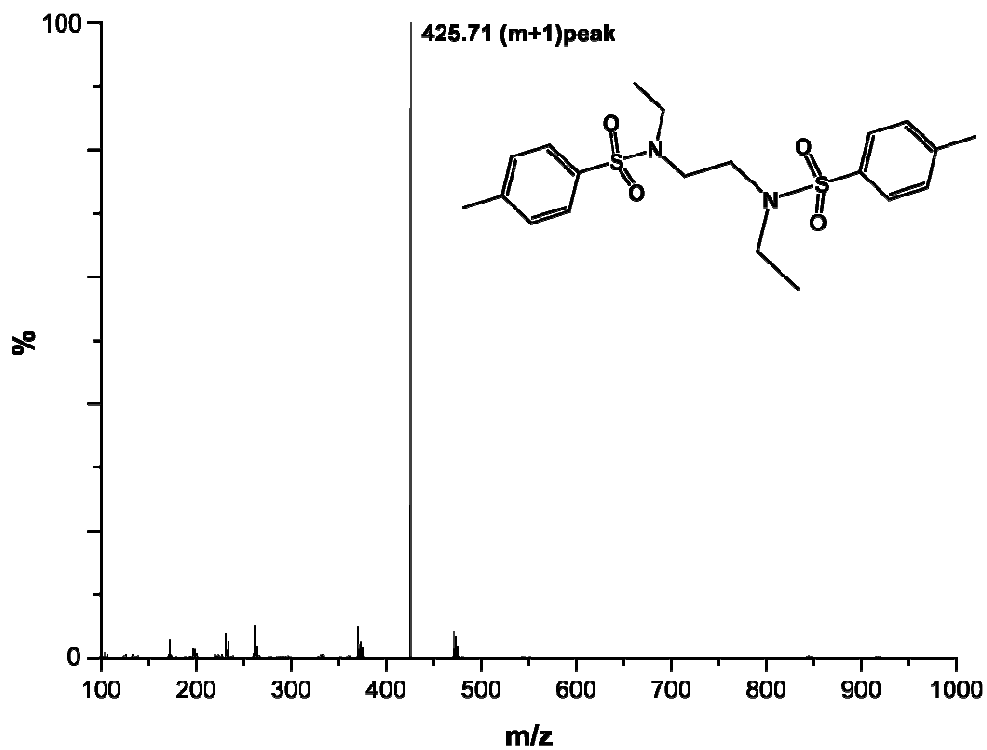


Figure S8: ESI-Mass spectrum of T-2 in methanol.

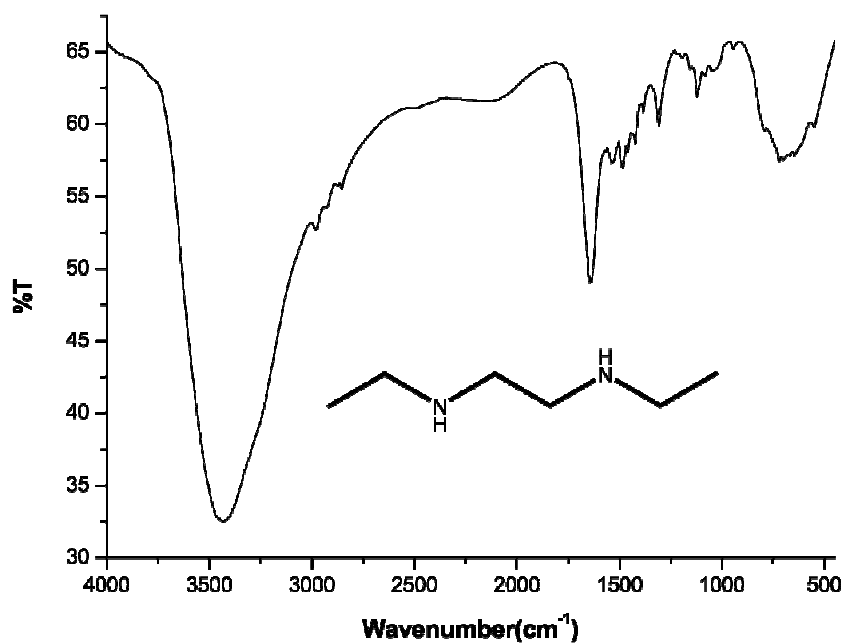


Figure S9: FT-IR spectrum of L<sub>2</sub> in KBr pellet.

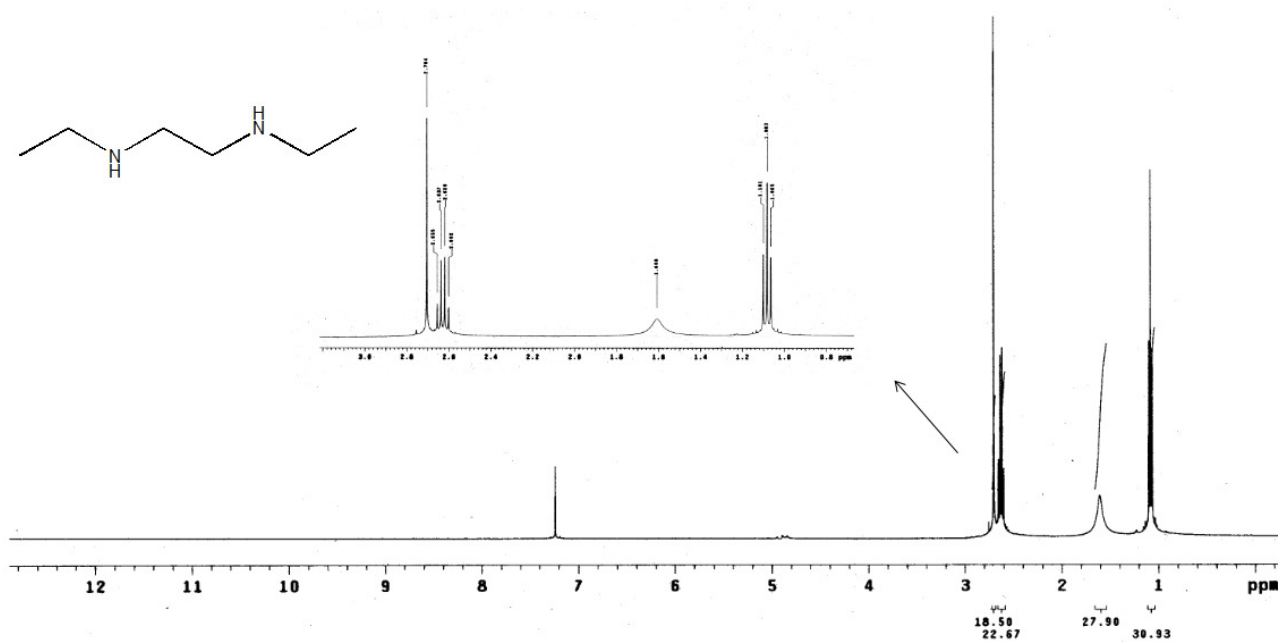


Figure S10: <sup>1</sup>H-NMR spectrum of L<sub>2</sub> in CDCl<sub>3</sub>.

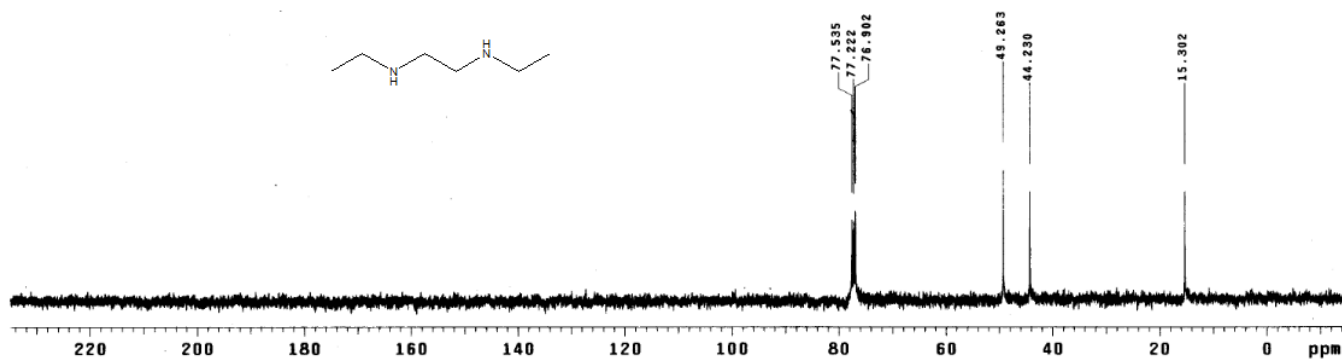


Figure S11:  $^{13}\text{C}$ -NMR spectrum of  $L_2$  in  $\text{CDCl}_3$ .

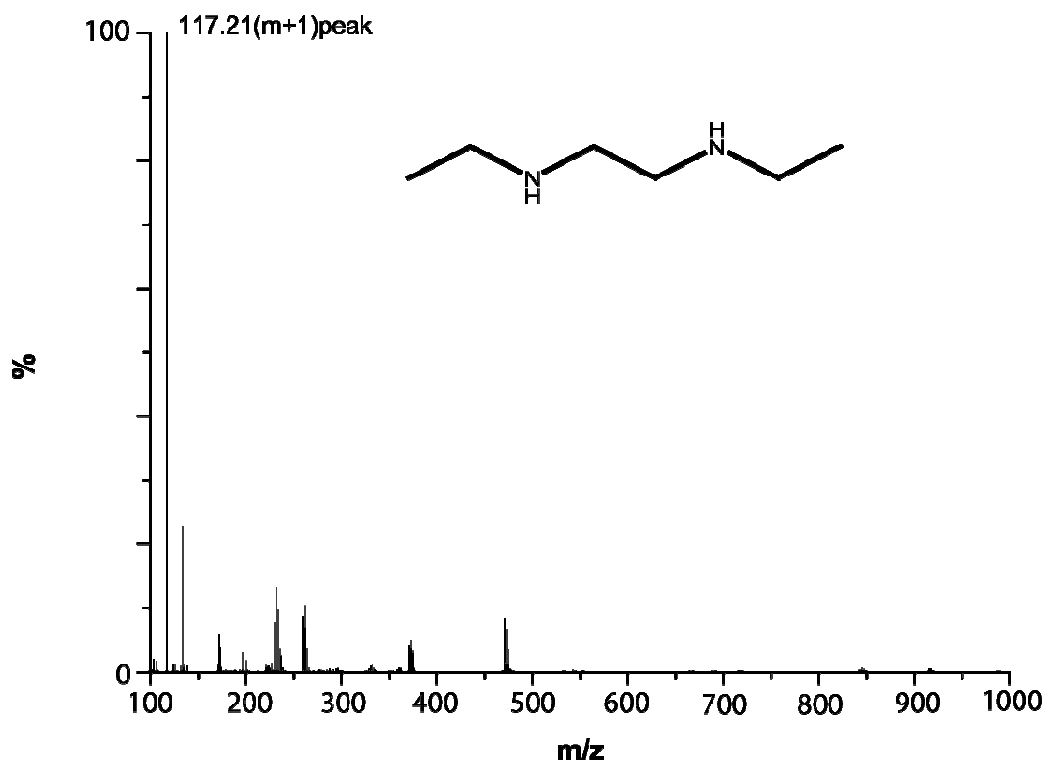
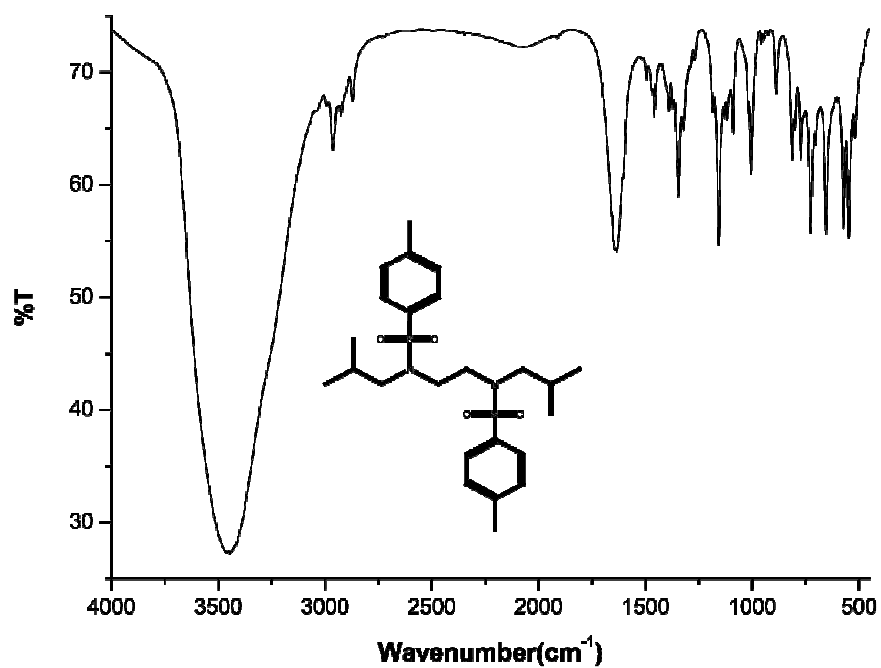
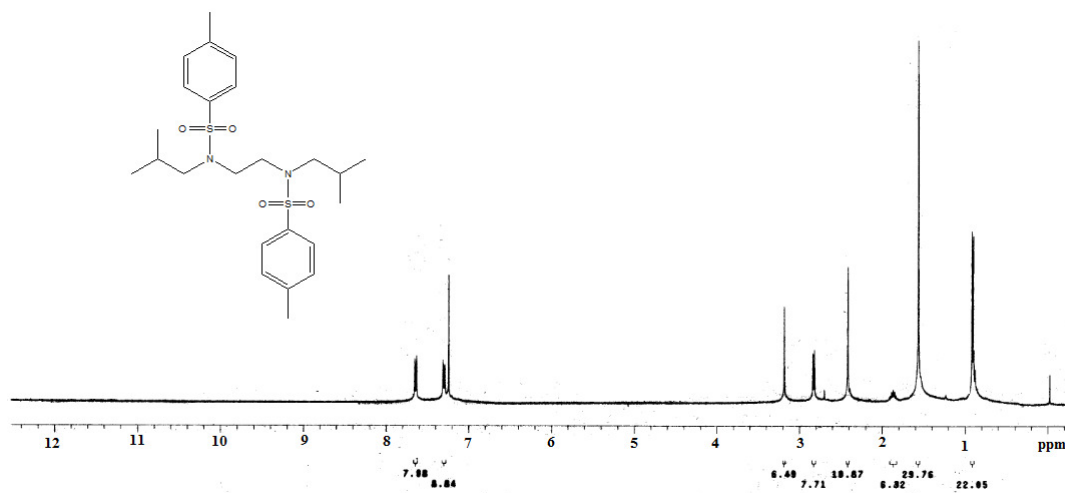


Figure S12: ESI-Mass spectrum of  $L_2$  in methanol.



**Figure S13:** FT-IR spectrum of T-3 in KBr pellet.



**Figure S14:** <sup>1</sup>H-NMR spectrum of T-3 in CDCl<sub>3</sub>.

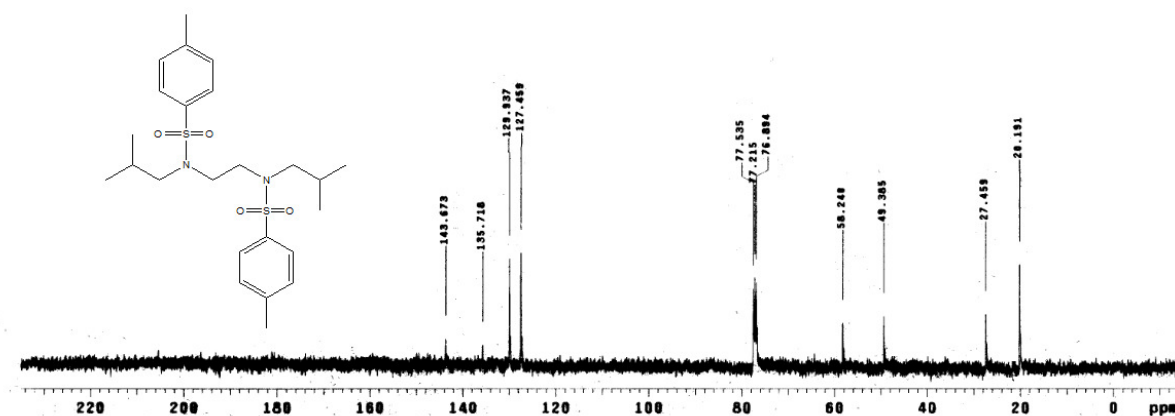


Figure S15:  $^{13}\text{C}$ -NMR spectrum of T-3 in  $\text{CDCl}_3$ .

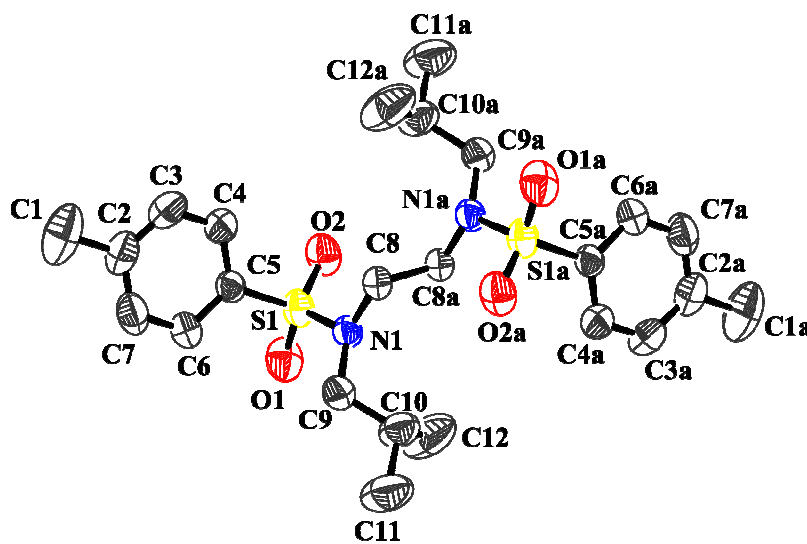


Figure S16: ORTEP diagram of T-3 [a (-x, 1-y, -z) symmetry transformation is implied by each additional atom level] (50% thermal ellipsoid plot).

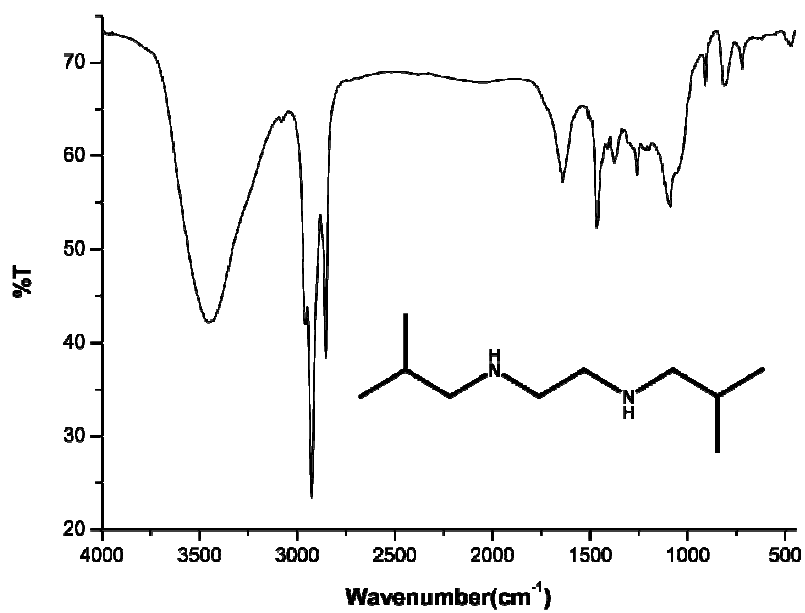


Figure S17: FT-IR spectrum of L<sub>3</sub> in KBr pellet.

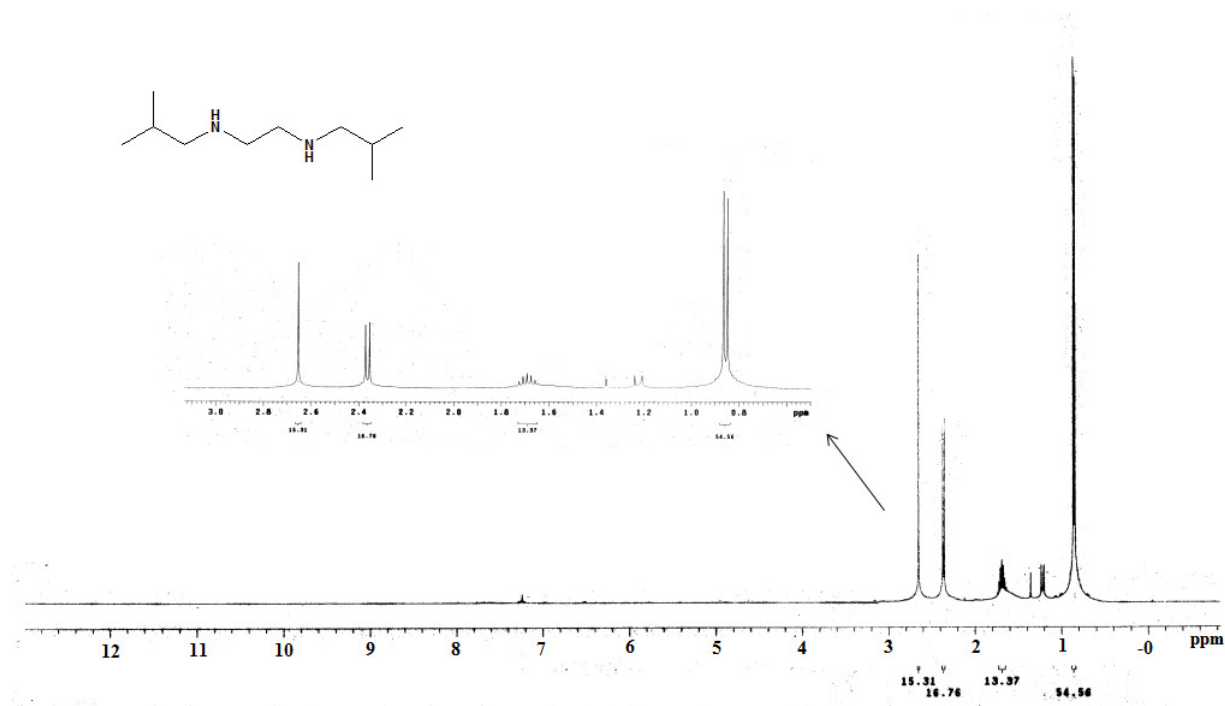


Figure S18: <sup>1</sup>H-NMR spectrum of L<sub>3</sub> in CDCl<sub>3</sub>.

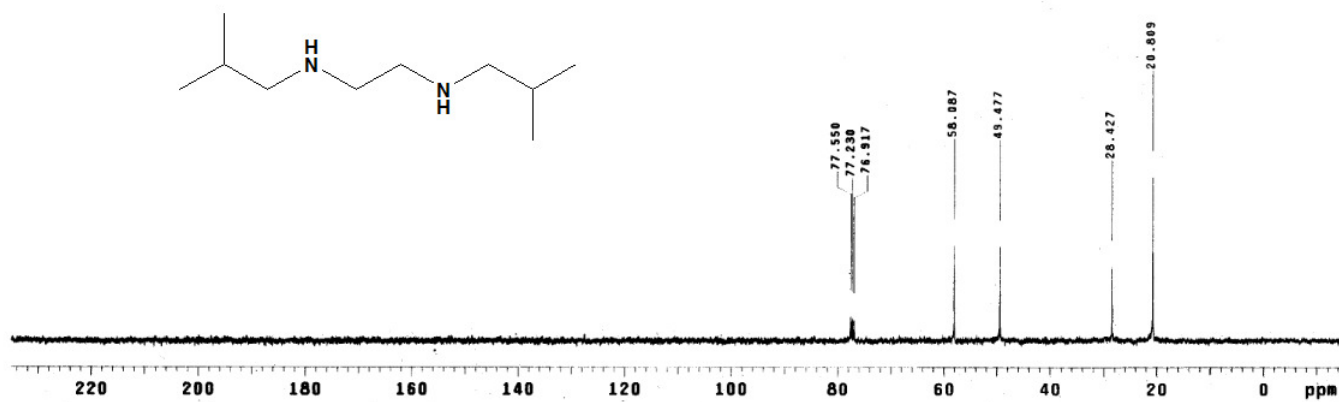


Figure S19:  $^{13}\text{C}$ -NMR spectrum of  $\text{L}_3$  in  $\text{CDCl}_3$ .

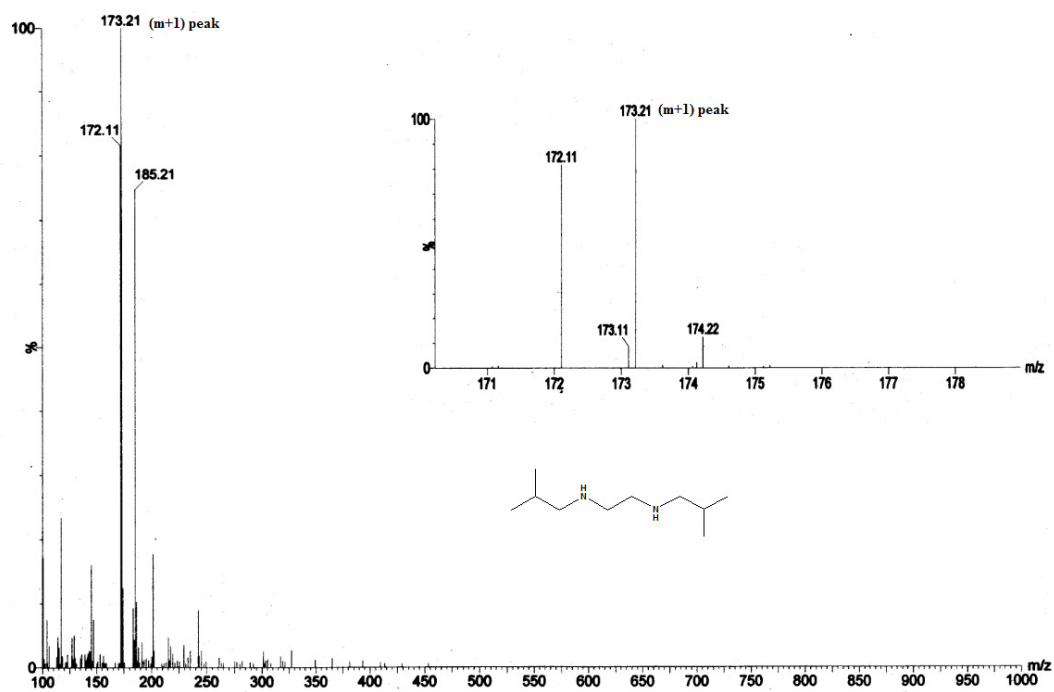
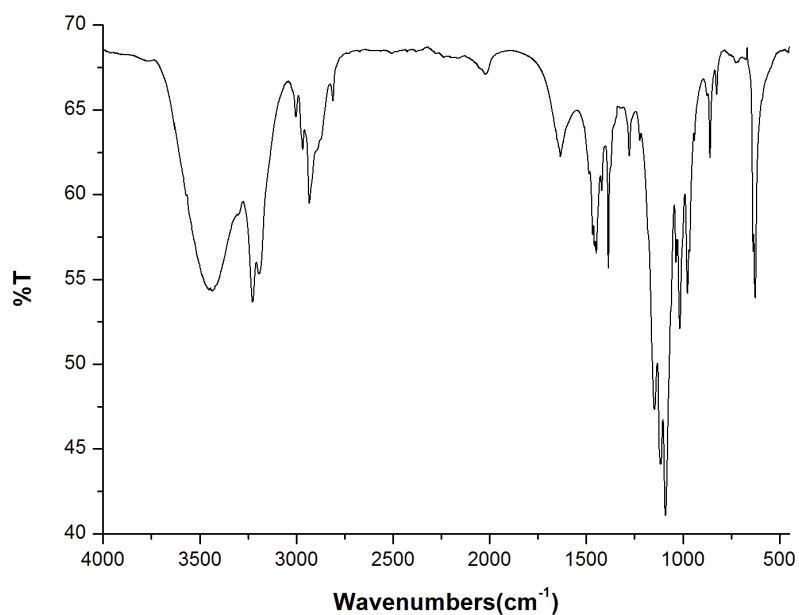
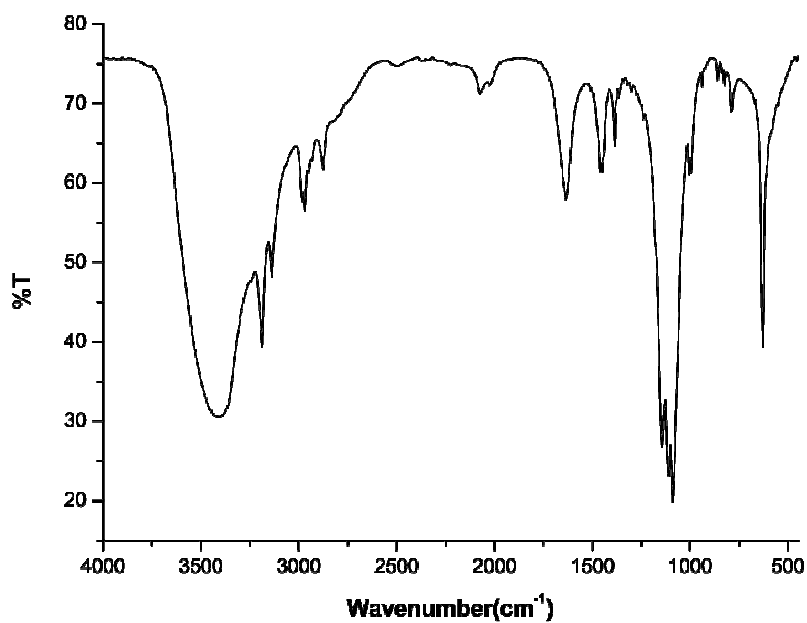


Figure S20: ESI-Mass spectrum of  $\text{L}_3$  in methanol.



**Figure S21:** FT-IR spectrum of complex **1** in KBr pellet.



**Figure S22:** FT-IR spectrum of complex **2** in KBr pellet.

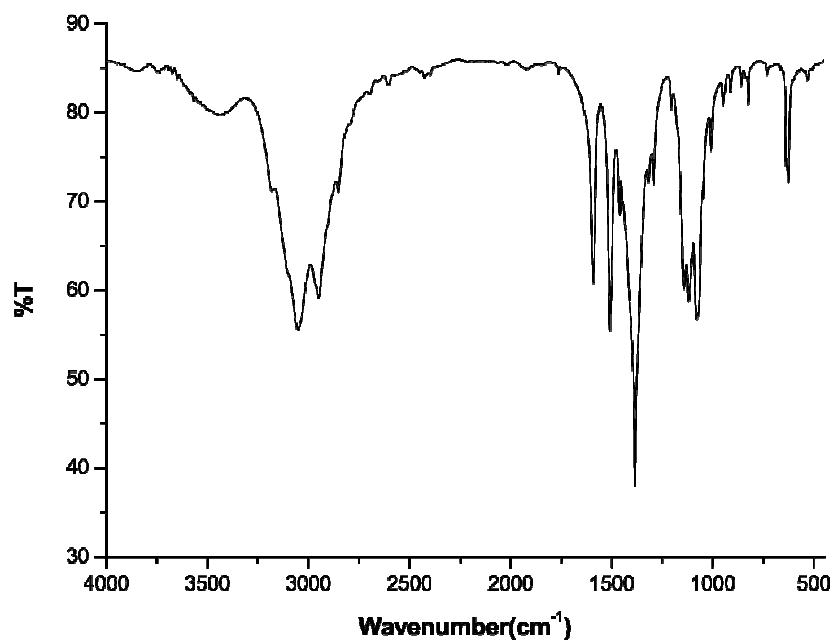
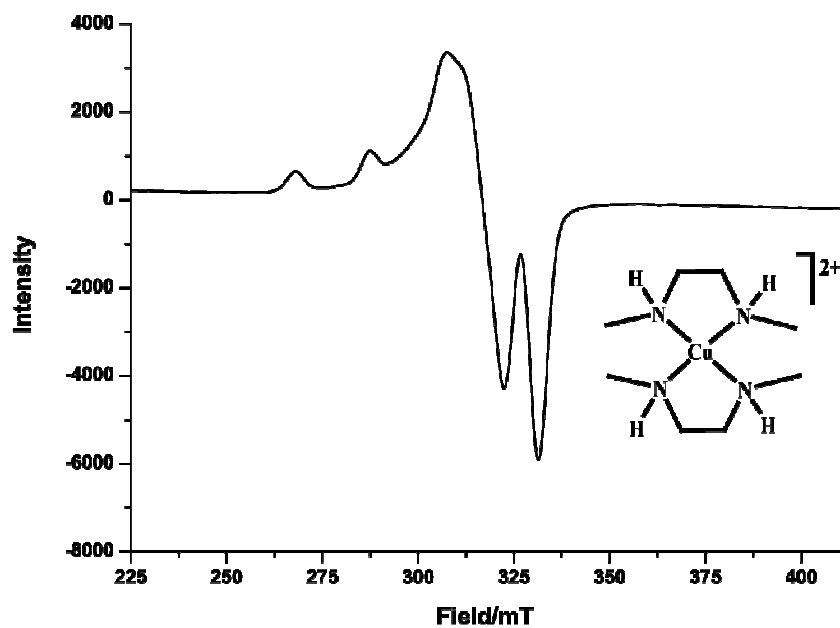
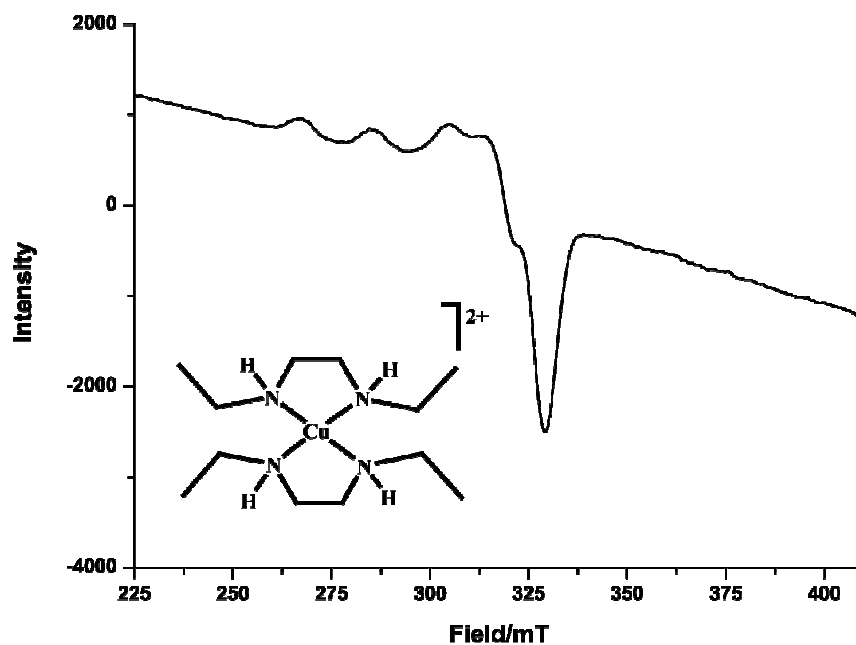


Figure S23: FT-IR spectrum of complex **3** in KBr pellet.



**Figure S24:** X-Band EPR spectrum of complex **1** in CH<sub>3</sub>CN/CH<sub>3</sub>OH(50% v/v) at 77K.  
Microwave power: 0.998 mW; microwave frequency: 9.14 GHz; modulation amplitude: 2;  
Receiver gain:  $2 \times 10^3$ ; Time constant: 0.03s.



**Figure S25:** X-Band EPR spectrum of complex **2** in CH<sub>3</sub>CN/CH<sub>3</sub>OH(50% v/v) at 77K.  
Microwave power: 0.998 mW; microwave frequency: 9.14 GHz; modulation amplitude: 2.  
Receiver gain:  $2 \times 10^3$ ; Time constant: 0.03s.



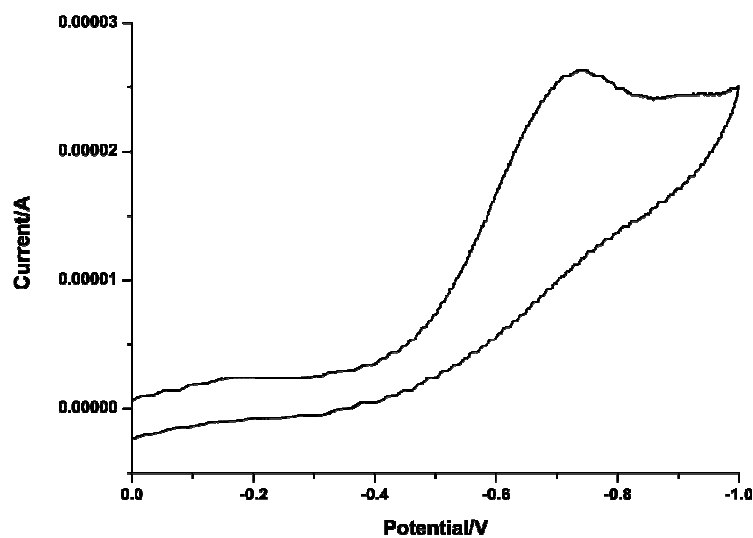


**Figure S28:** Cyclic voltammogram of complex **2** in acetonitrile. (Tetrabutylammonium perchlorate supporting electrolyte; Pt working and SCE reference electrode and 50 mv/s scan rate).

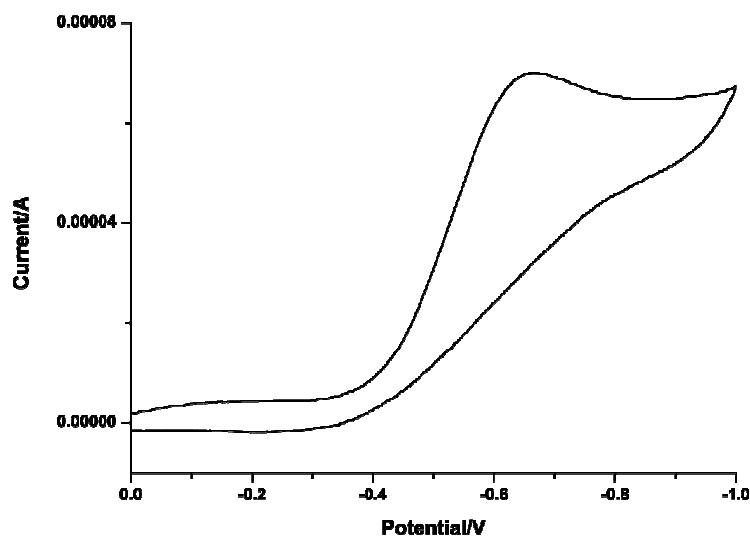


**Figure S29:** Cyclic voltammogram of complex **3** in acetonitrile. (Tetrabutylammonium perchlorate supporting electrolyte; Pt working and SCE reference electrode and 50 mv/s scan rate).

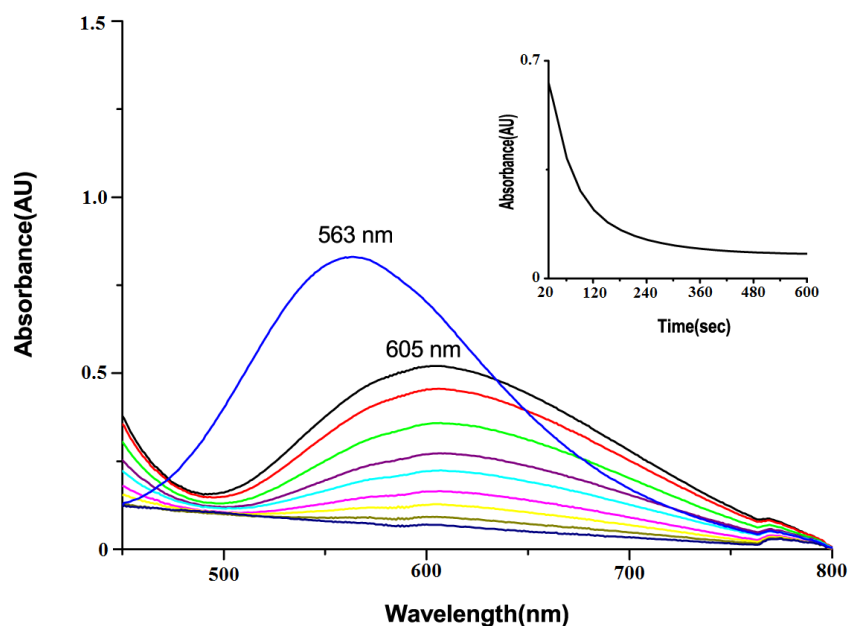


**Figure S30:** UV-visible spectra of the reaction of complexes **1** with nitric oxide in acetonitrile solvent at room temperature. (Blue trace represents the  $\text{Cu}^{\text{II}}$ -species, black represents that of the  $[\text{Cu}^{\text{II}}\text{-NO}]$  intermediate which gradually reduced to  $\text{Cu}^{\text{I}}$ -species). {Inset: time scan plots at 605 nm}.

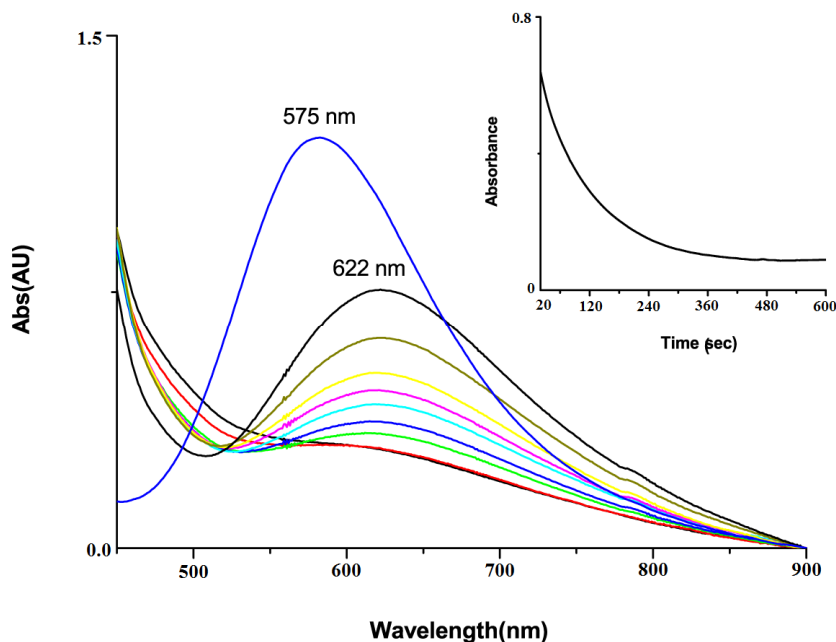


**Figure S31:** UV-visible spectra of the reaction of complexes **2** with nitric oxide in acetonitrile solvent at room temperature. (Blue trace represents the  $\text{Cu}^{\text{II}}$ -species, black represents that of the

[Cu<sup>II</sup>-NO] intermediate which gradually reduced to Cu<sup>I</sup>-species). {Inset: time scan plots at 622 nm}.

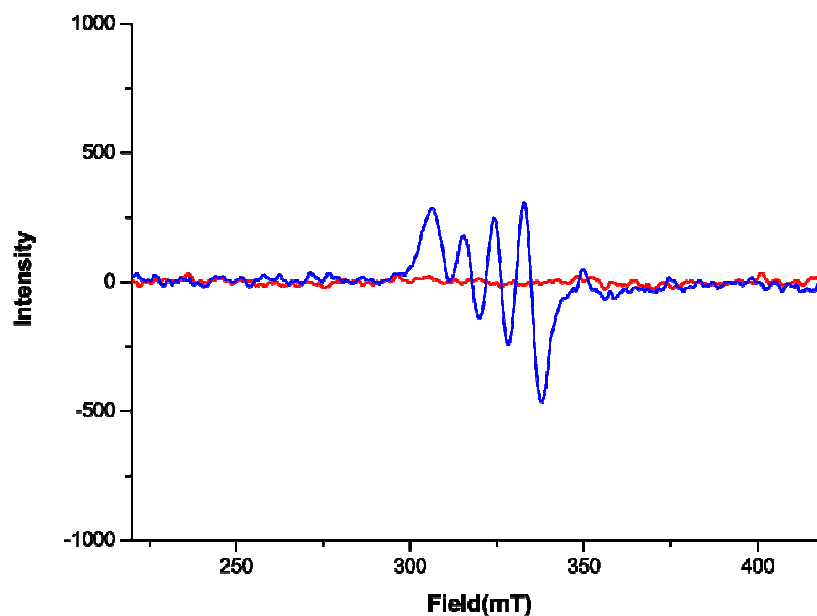


**Figure S32:** X-Band EPR spectra of complex **1** before (blue trace) and after (red trace) purging NO in acetonitrile at room temperature.

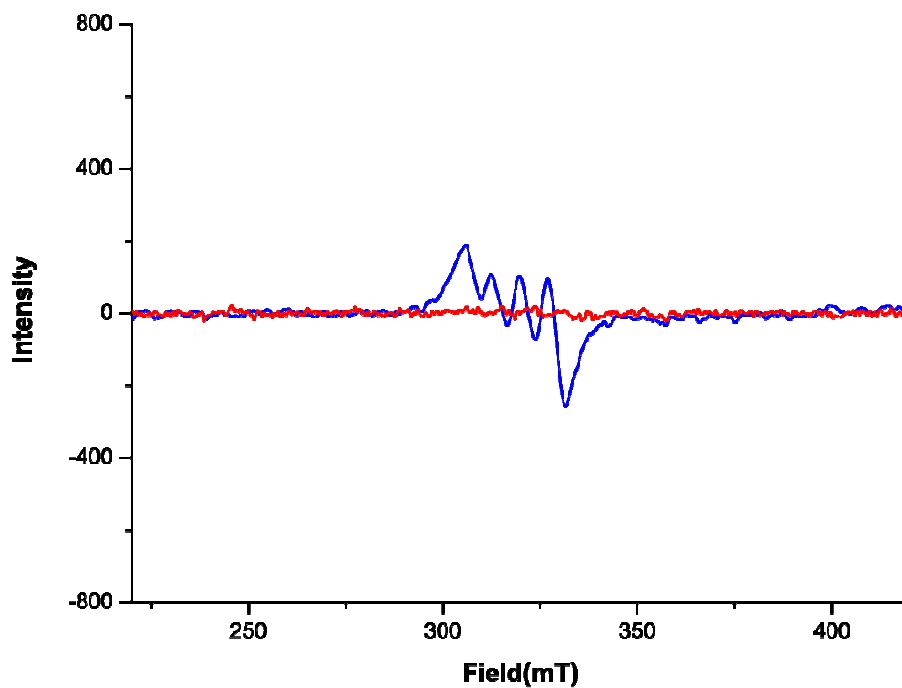


**Figure S33:** X-Band EPR spectra of complex **2** before (blue trace) and after (red trace) purging NO in acetonitrile at room temperature.

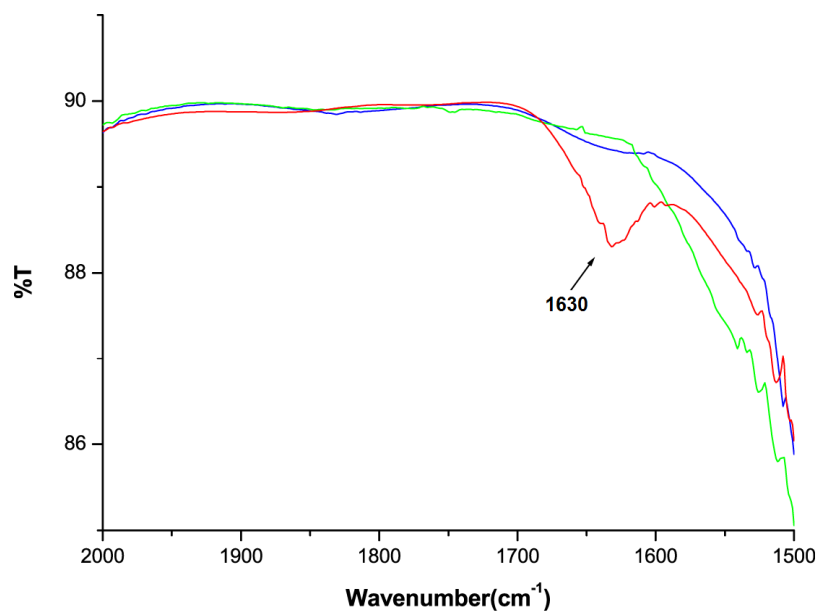


**Figure S34:** Solution FT-IR spectra complex **2** in acetonitrile. (Blue trace represents solution FT-IR spectrum of complex **2**, red represents that immediately after purging nitric oxide which shows peak at  $1630\text{ cm}^{-1}$  and green represents that after 10 minutes.).

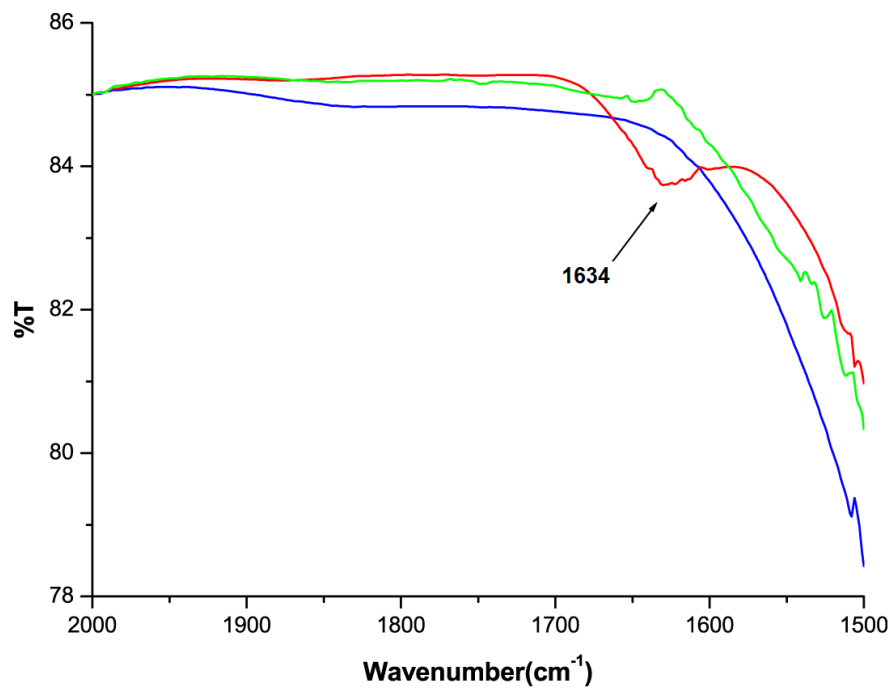


**Figure S35:** Solution FT-IR spectra complex **3** in acetonitrile. (Blue trace represents solution FT-IR spectrum of complex **3**, red represents that immediately after purging nitric oxide and green represents that after 10 minutes).

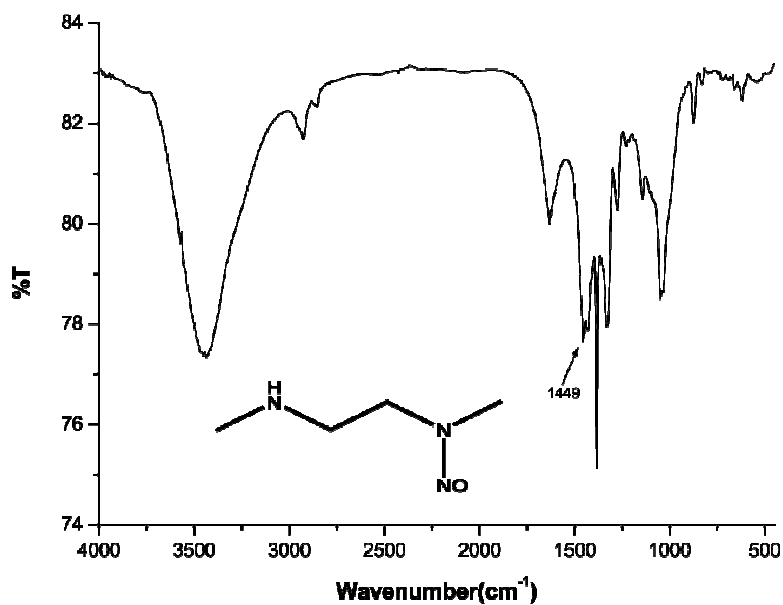


**Figure S36:** FT-IR spectrum of  $L_1$  in KBr pellet.

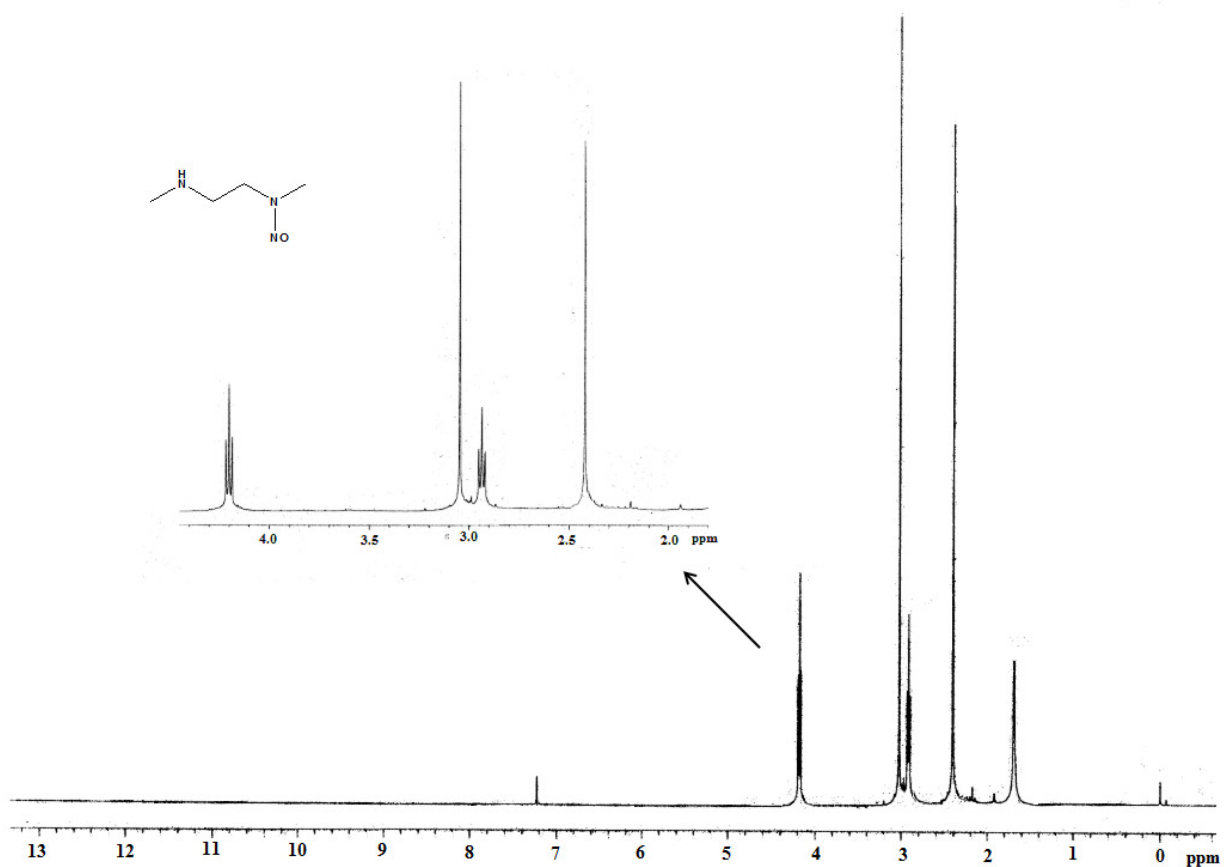


Figure S37: <sup>1</sup>H-NMR spectrum of L<sub>1</sub>' of in CDCl<sub>3</sub>.

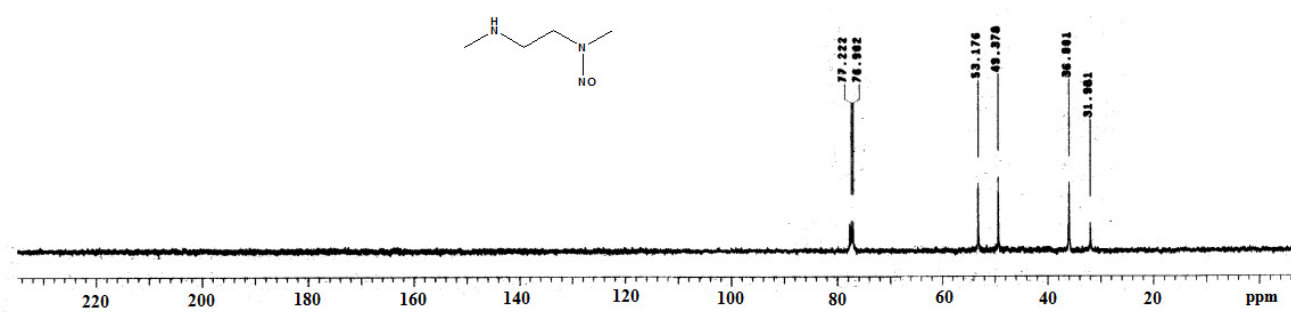


Figure S38: <sup>13</sup>C-NMR spectrum of L<sub>1</sub>' of in CDCl<sub>3</sub>.

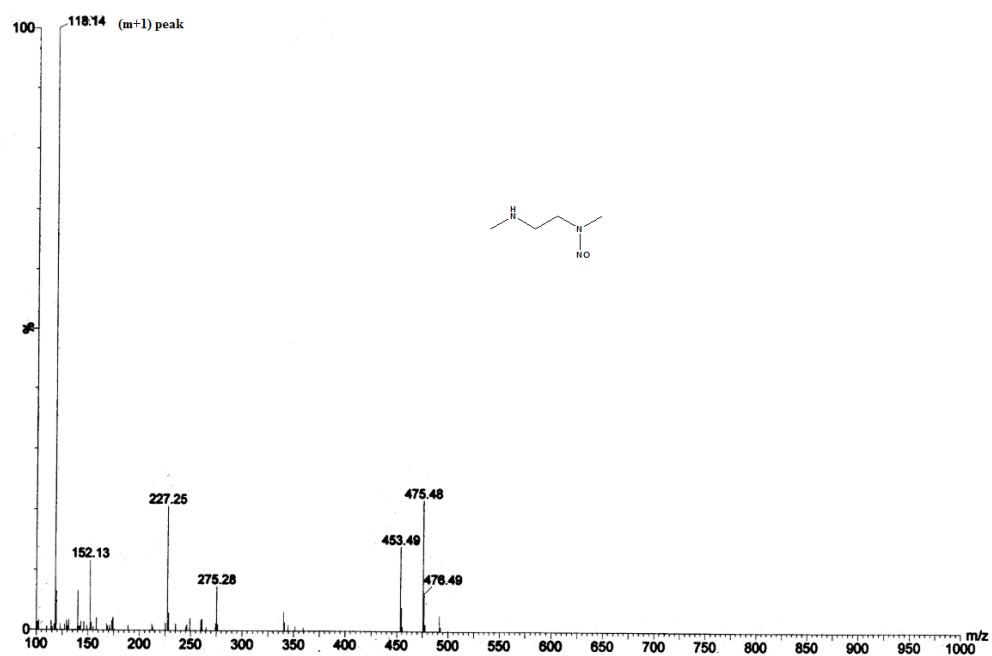


Figure S39: ESI-mass spectrum of  $L_1'$  in methanol.

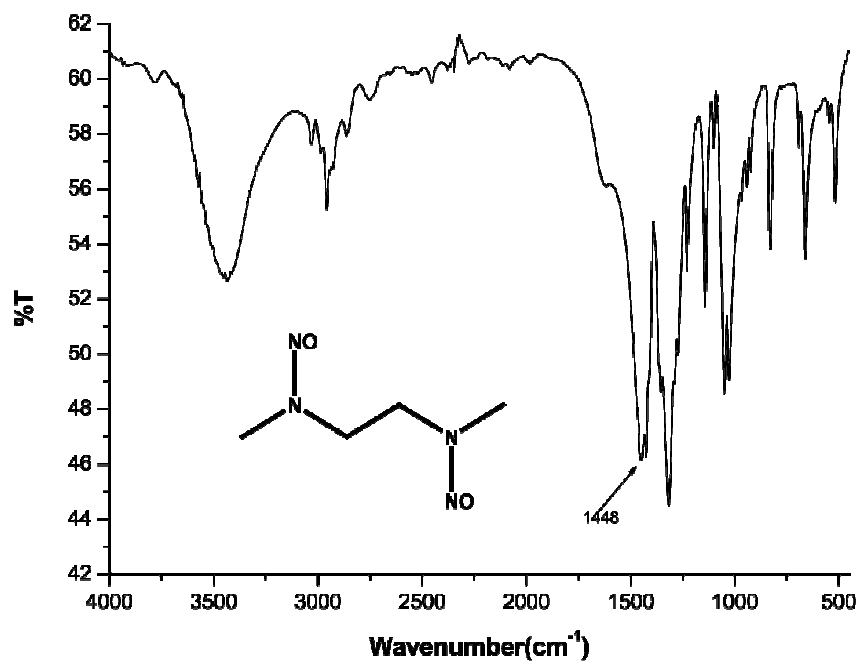
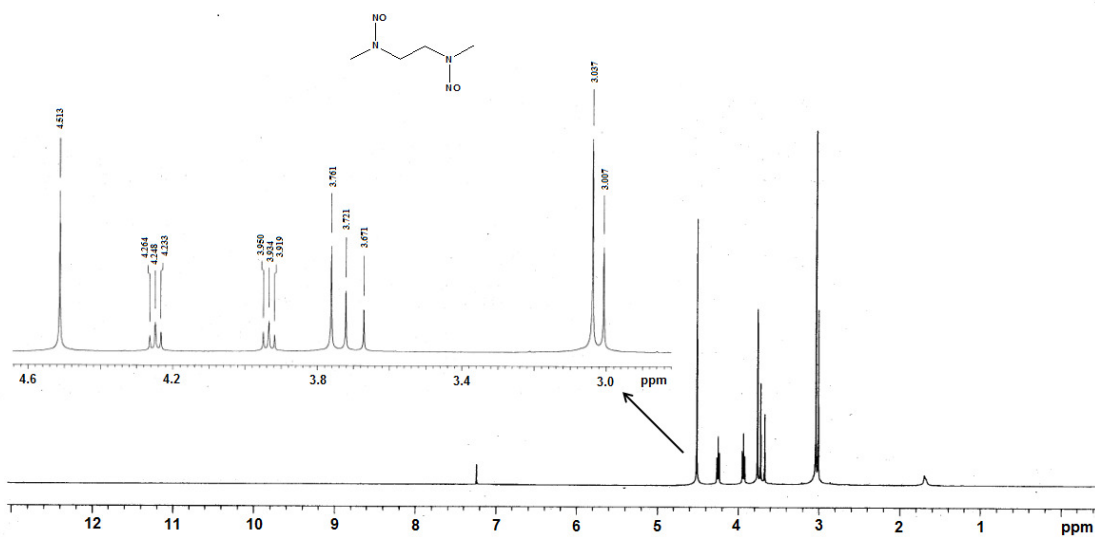
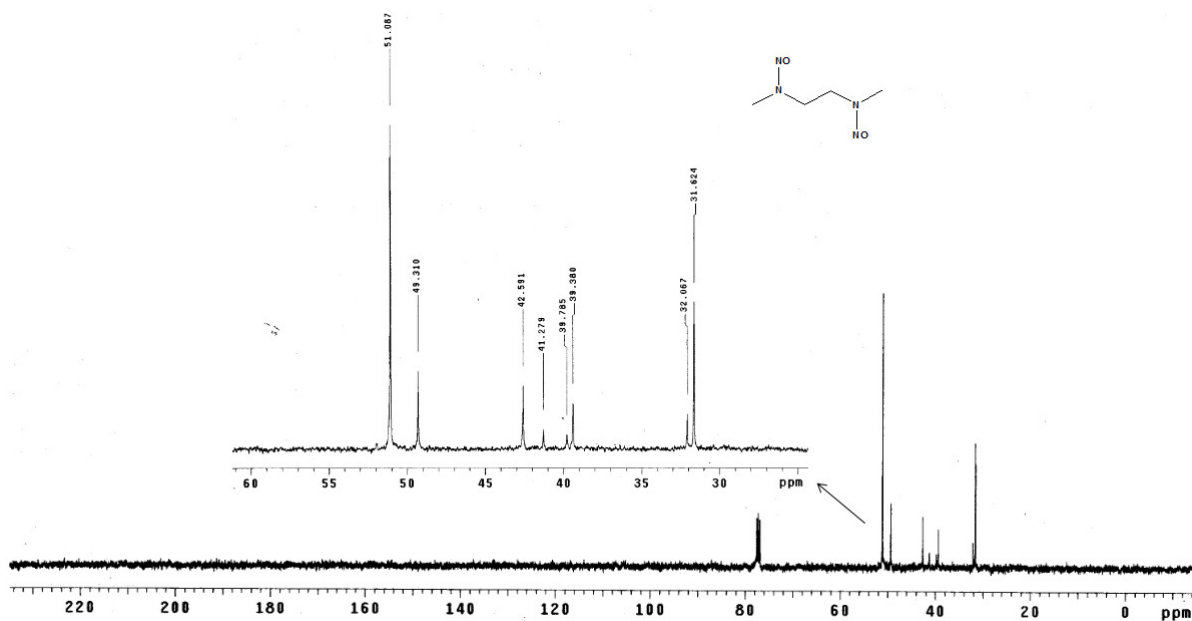


Figure S40: FT-IR spectrum of  $L_1''$  in KBr pellet.



**Figure S41:** <sup>1</sup>H-NMR spectrum of L<sub>1</sub> in CDCl<sub>3</sub>. The presence of extra signals in <sup>1</sup>H- and <sup>13</sup>C-NMR spectra are due to isomeric impurities.<sup>1</sup>



**Figure S42:** <sup>13</sup>C-NMR spectrum of L<sub>1</sub> in CDCl<sub>3</sub>. The presence of extra signals in <sup>1</sup>H- and <sup>13</sup>C-NMR spectra are due to isomeric impurities.<sup>1</sup>

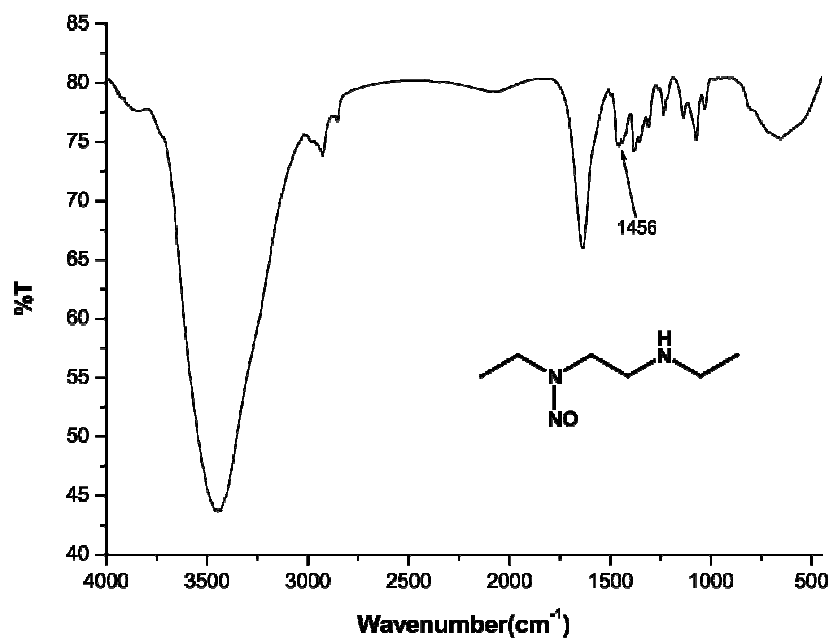


Figure S43: FT-IR spectrum of L<sub>2</sub>' in KBr pellet.

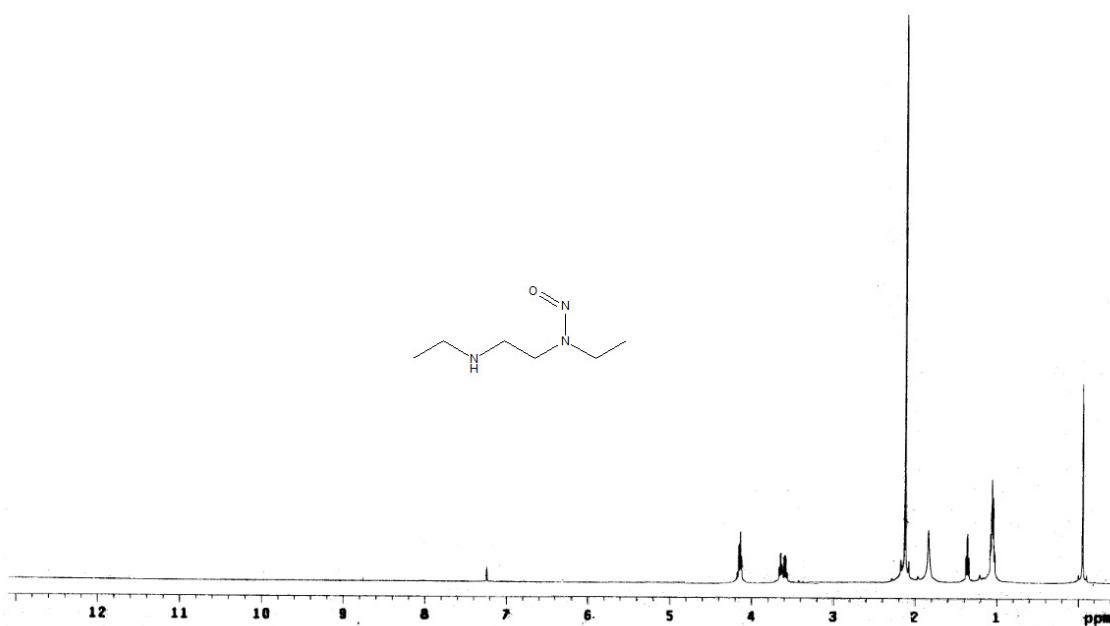


Figure S44: <sup>1</sup>H-NMR spectrum of L<sub>2</sub>' of in CDCl<sub>3</sub>.

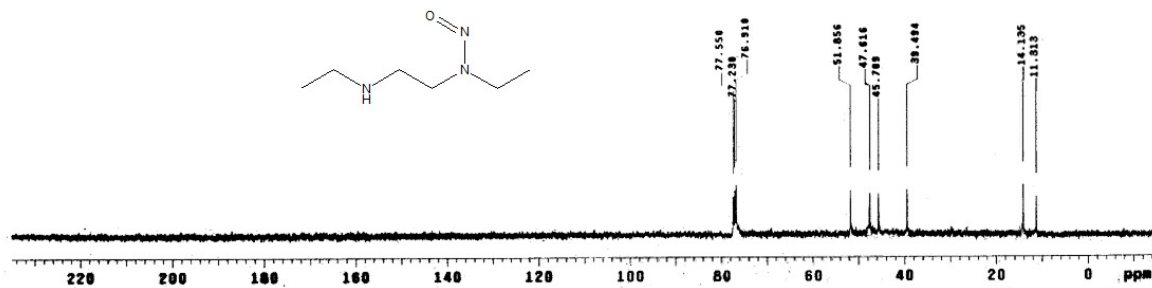


Figure S45:  $^{13}\text{C-NMR}$  spectrum of  $L_2'$  in  $\text{CDCl}_3$ .

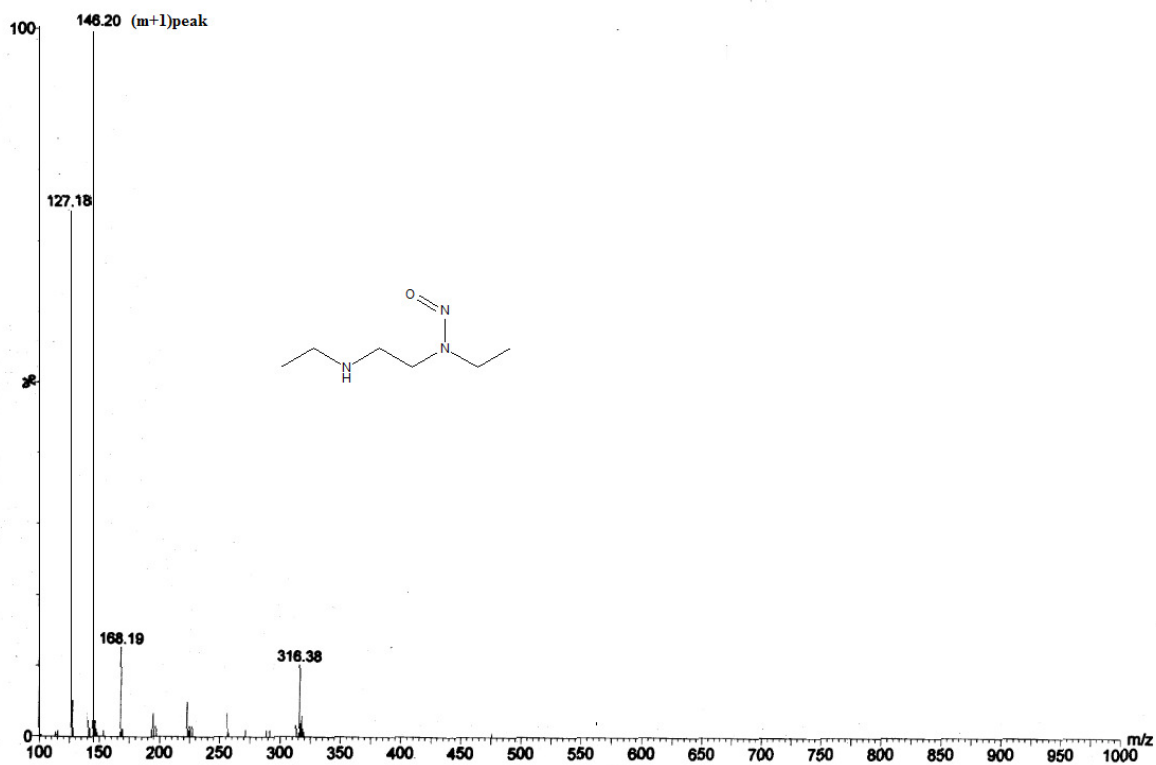


Figure S46: ESI-mass spectrum of  $L_2'$  in methanol.

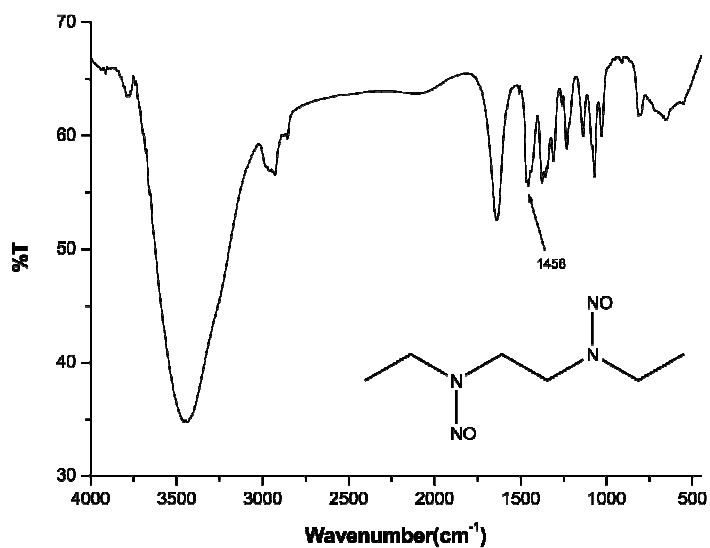


Figure S47: FT-IR spectrum of  $L_2''$  in KBr pellet.

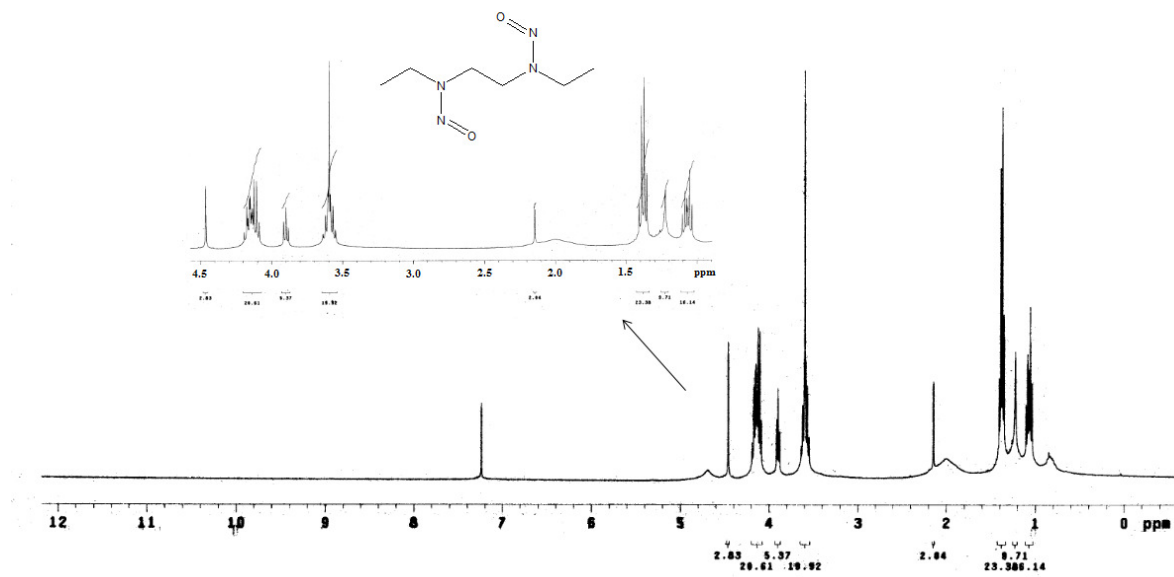
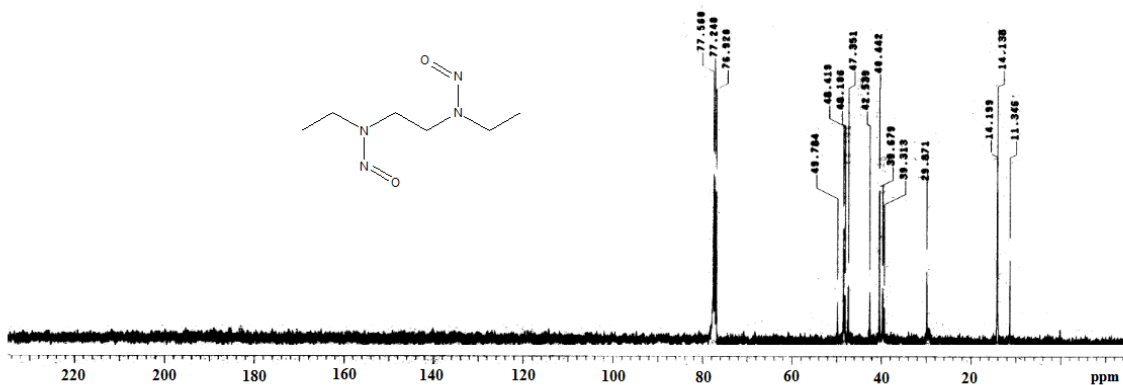
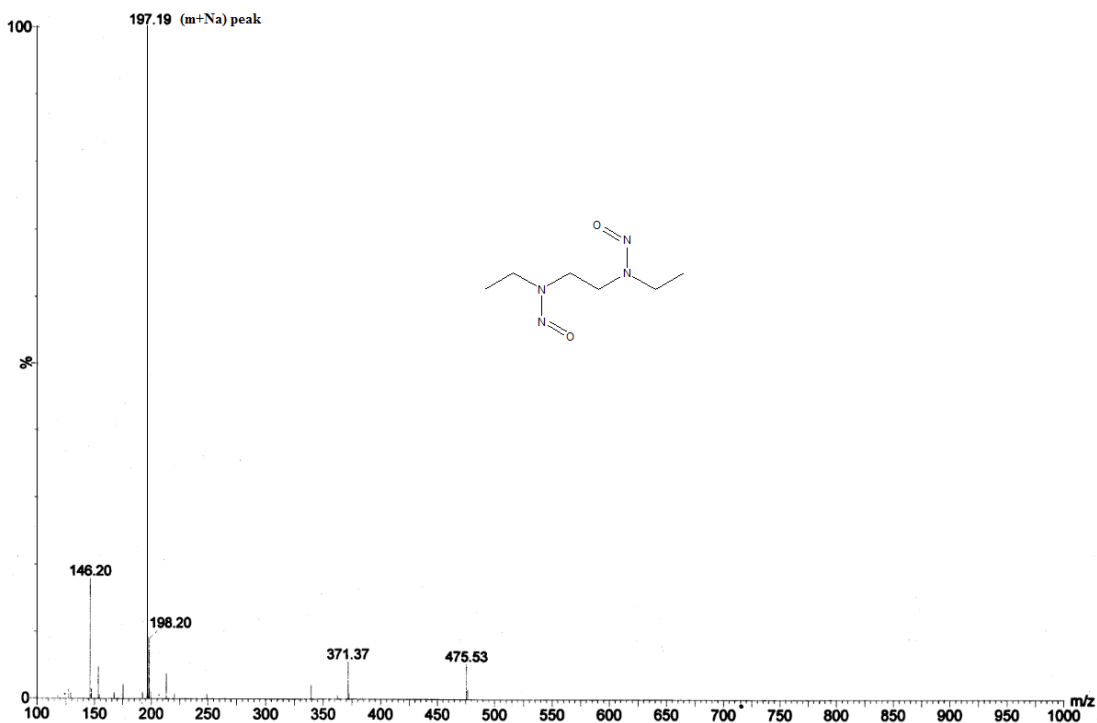


Figure S48:  $^1\text{H-NMR}$  spectrum of  $L_2''$  of in  $\text{CDCl}_3$ . The presence of extra signals in  $^1\text{H-}$  and  $^{13}\text{C-}$  NMR spectra are due to isomeric impurities.<sup>1</sup>



**Figure S49:**  $^{13}\text{C}$ -NMR spectrum of  $\text{L}_2''$  of in  $\text{CDCl}_3$ . The presence of extra signals in  $^1\text{H}$ - and  $^{13}\text{C}$ - NMR spectra are due to isomeric impurities.<sup>1</sup>



**Figure S50:** ESI-Mass spectrum of  $\text{L}_2''$  in methanol.

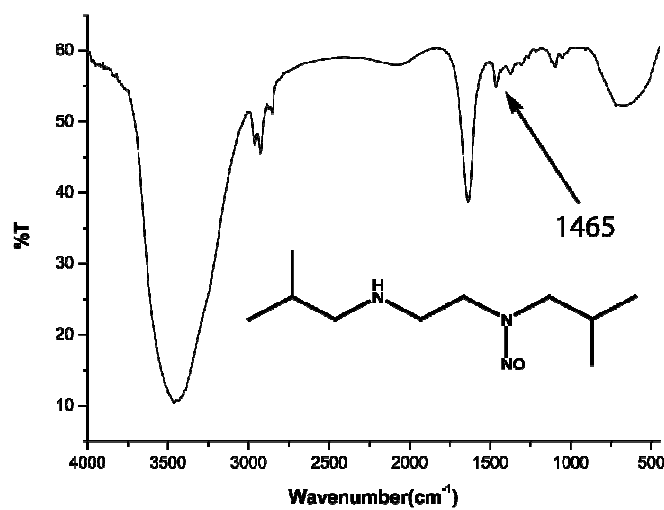


**Figure S51:** FT-IR spectrum of  $L_3$  in KBr pellet.

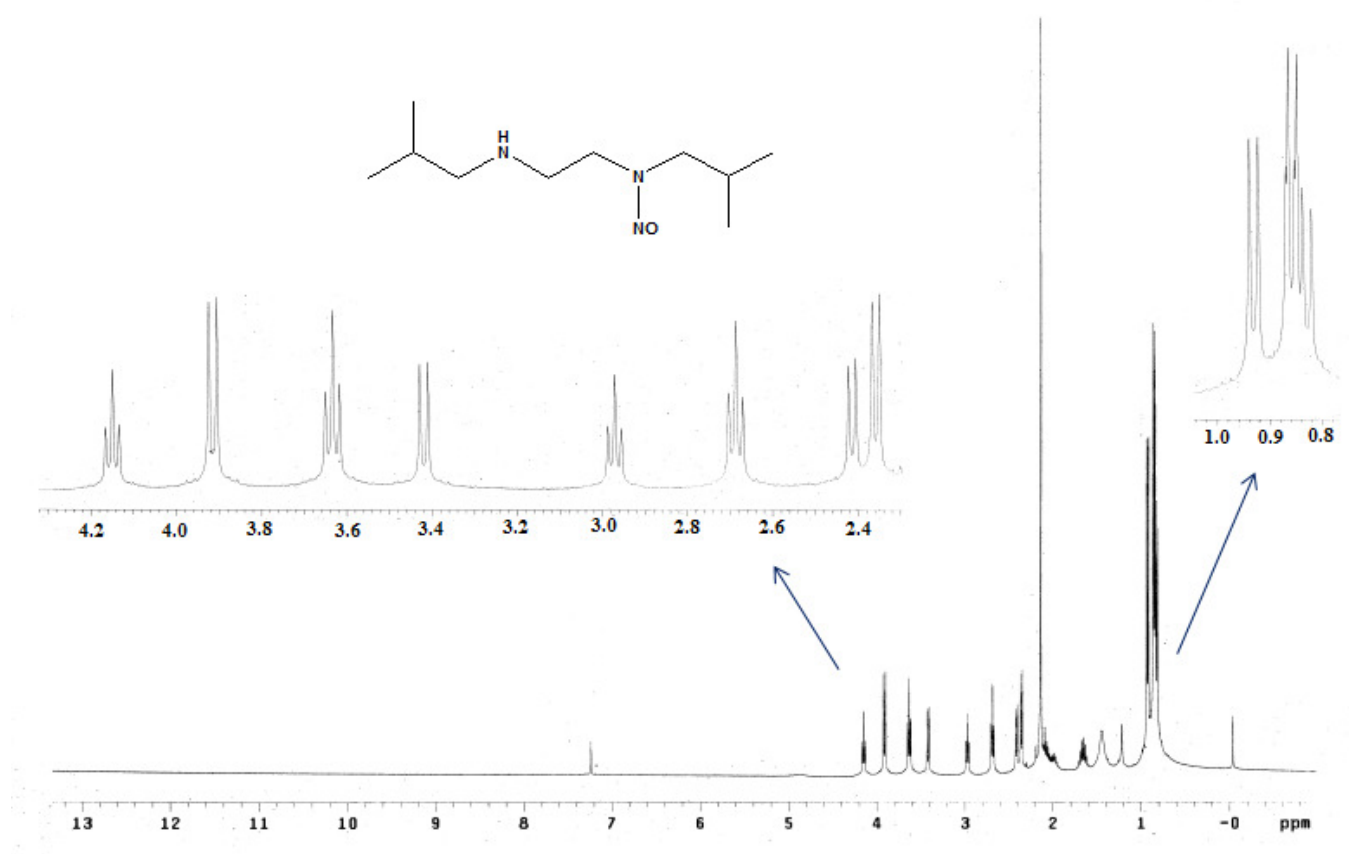
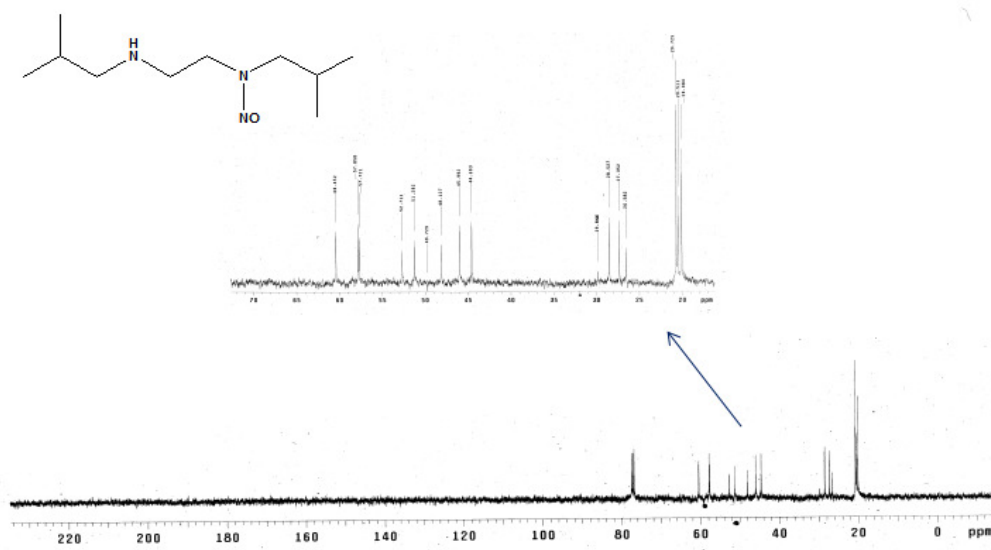


**Figure S52:**  $^1\text{H-NMR}$  spectrum of  $L_3$  in  $\text{CDCl}_3$ . The presence of extra signals in  $^1\text{H-}$  and  $^{13}\text{C-}$  NMR spectra are due to isomeric impurities.<sup>1</sup>



**FigureS53:** <sup>13</sup>C-NMR spectrum of L<sub>3</sub>' of in CDCl<sub>3</sub>. The presence of extra signals in <sup>1</sup>H- and <sup>13</sup>C-NMR spectra are due to isomeric impurities.<sup>1</sup>

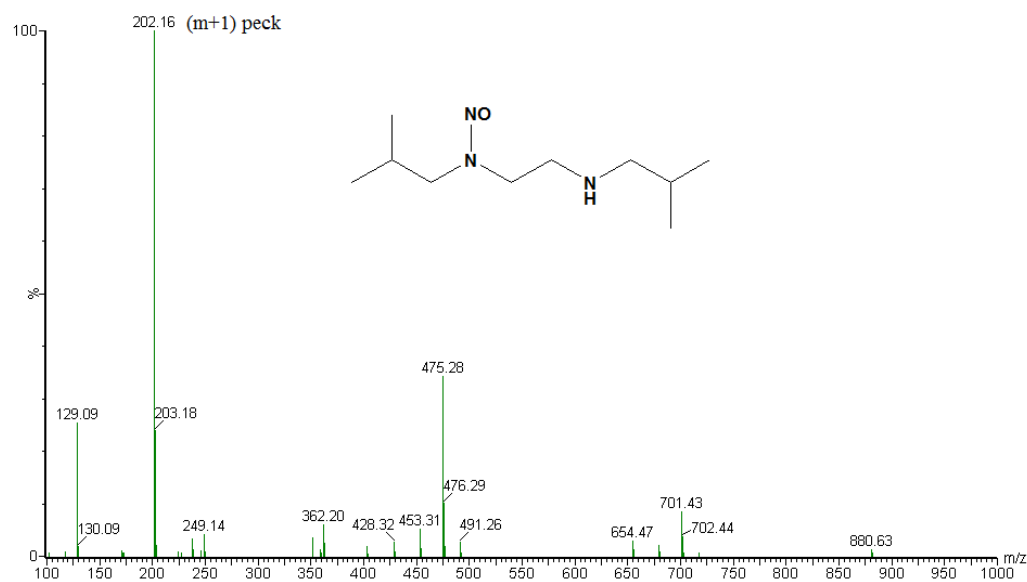


**Figure S54:** ESI-Mass spectrum of L<sub>3</sub>' in methanol.

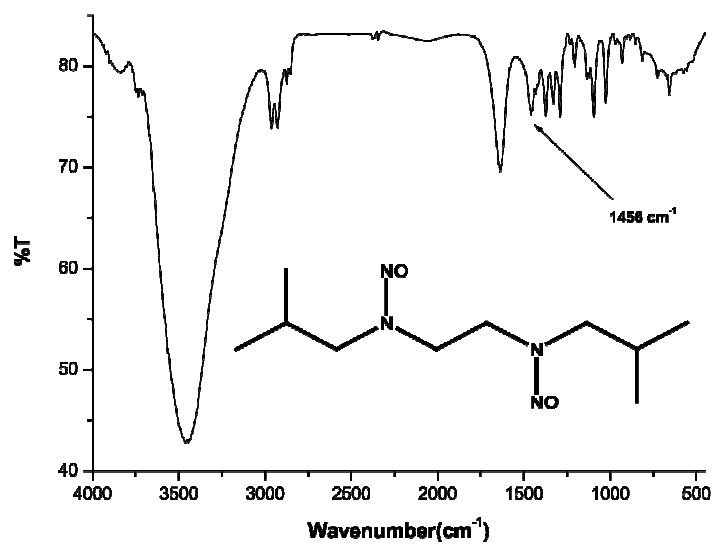


Figure S55: FT-IR spectrum of  $L_3''$  in KBr pellet.

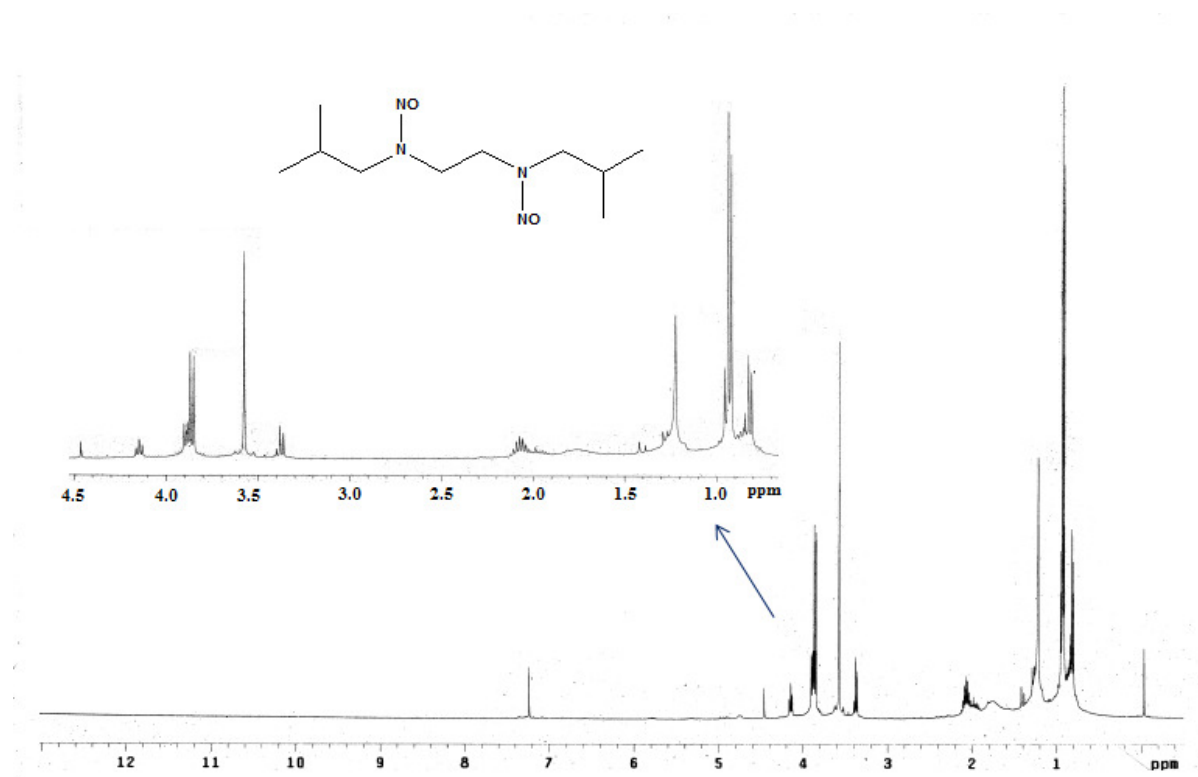


Figure S56:  $^1\text{H-NMR}$  spectrum of  $L_3''$  in  $\text{CDCl}_3$ .

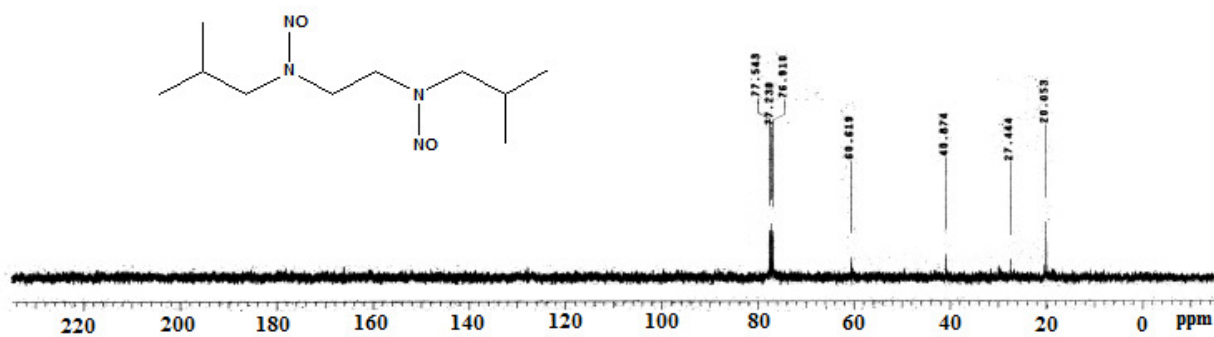


Figure S57:  $^{13}\text{C}$ -NMR spectrum of  $L_3''$  in  $\text{CDCl}_3$ .

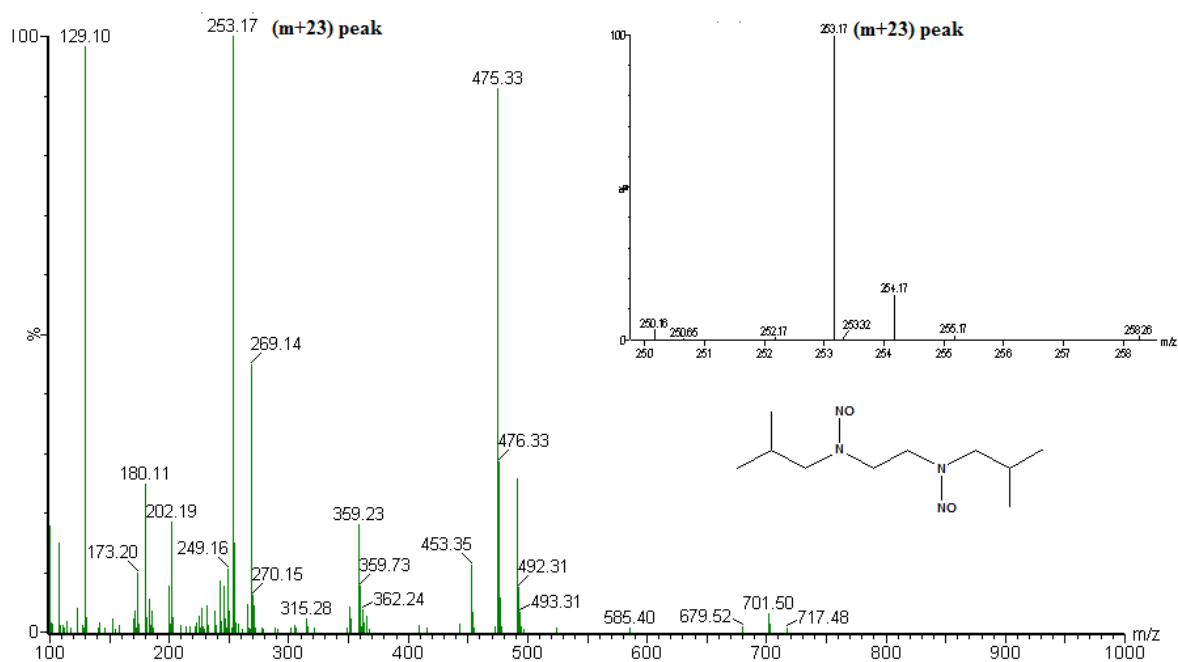


Figure S58: ESI-Mass spectrum of  $L_3''$  in methanol.

**Table S1.** Crystallographic data for  $L_1^{II}$ .

	ligand
Formulae	$C_4 H_{10} N_4 O_2$
Mol. wt.	146.16
Crystal system	Monoclinic
Space group	C2/c
Temperature /K	296(2)
Wavelength /Å	0.71073
$a / \overset{\circ}{\text{Å}}$	5.7944(6)
$b / \overset{\circ}{\text{Å}}$	10.0079(6)
$c / \overset{\circ}{\text{Å}}$	13.3326(11)
$\alpha / ^\circ$	90.00
$\beta / ^\circ$	97.710(6)
$\gamma / ^\circ$	90.00
$V / \overset{\circ}{\text{Å}}^3$	766.16(11)
Z	4
Density/Mgm <sup>-3</sup>	1.267
Abs. Coeff. /mm <sup>-1</sup>	0.102
Abs. correction	None
F(000)	312
Total no.of reflections	879
Reflections, $I > 2\sigma(I)$	482
Max. $2\theta / ^\circ$	27.43
Ranges (h, k, l)	-5 ≤ h ≤ 7 -12 ≤ k ≤ 7 -17 ≤ l ≤ 17
Complete to $2\theta$ (%)	99.8%
Refinement method	Full-matrix least-squares on $F^2$
Goof ( $F^2$ )	1.145
<b>Rint</b>	<b>0.0698</b>
R indices [ $I > 2\sigma(I)$ ]	0.0638
R indices (all data)	0.0984

**Table S2:** Selected bond length (Å) and angle (°) of  $L_1^{II}$ .

Bond lengths(Å)		Bond angles (°)	
N1-N2	1.323(3)	N1-N2-O1	112.8(3)
N2-O1	1.220(4)	N2-N1-C1	115.2(2)
N1-C1	1.442(3)	N2-N1-C2	122.1(2)

N1-C2	1.442(3)	-	-
-------	----------	---	---

**Table S3: Crystallographic Data for ligand T-3.**

	<b>Ligand T-3</b>
Formulae	C <sub>24</sub> H <sub>36</sub> N <sub>2</sub> S <sub>2</sub> O <sub>4</sub>
Mol. wt.	480.67
Crystal system	Triclinic
Space group	P-1
Temperature /K	296(2)
Wavelength /Å	0.71073
<i>a</i> /Å	5.3633(2)
<i>b</i> /Å	9.9606(5)
<i>c</i> /Å	12.5886(5)
$\alpha$ /°	91.902(3)
$\beta$ /°	98.241(3)
$\gamma$ /°	97.192(3)
<i>V</i> / Å <sup>3</sup>	659.43(5)
<i>Z</i>	1
Density/Mgm <sup>-3</sup>	1.210
Abs. Coeff. /mm <sup>-1</sup>	0.232
Abs. correction	None
F(000)	258
Total no. of reflections	2151
Reflections, <i>I</i> > 2σ( <i>I</i> )	1545
Max. 2θ/°	25.00
Ranges (h, k, l)	-6 ≤ h ≤ 6 -10 ≤ k ≤ 11 -14 ≤ l ≤ 14
Complete to 2θ (%)	92.5%
Refinement method	Full-matrix least-squares on <i>F</i> <sup>2</sup>
Goof ( <i>F</i> <sup>2</sup> )	1.024
<b>R<sub>int</sub></b>	<b>0.0683</b>
R indices [ <i>I</i> > 2σ( <i>I</i> )]	0.0444
R indices (all data)	0.0611

### Synthesis of copper(II) complex with tetramethylethylenediamine, Complex 4

Copper(II)perchlorate hexahydrate,  $[\text{Cu}(\text{H}_2\text{O})_6](\text{ClO}_4)_2$  (370 mg, 1.0 mmol) was dissolved in 10 ml of freshly distilled acetonitrile and to this blue solution, the ligand **L1**, *N,N'*-dimethyl ethylenediamine (232.2 mg, 2.0 mmol), was added drop wise. The color of the solution changed to violet. The resulting mixture was stirred for 1 h. Then the volume of the solution was reduced to ~2 ml and layered with benzene. Storage of this at ~ -20 °C overnight resulted in the precipitation of blue crystalline compound. Yield: 350 mg (~ 70%). Elemental Analyses: Calcd.(%) for  $\text{C}_{12}\text{H}_{32}\text{N}_4\text{O}_8\text{Cl}_2\text{Cu}$ : C, 29.12; H, 6.47; N, 11.32. Found (%) C, 29.14; H, 6.46; N, 11.27. UV-vis. (acetonitrile):  $\lambda_{\text{max}}$ , 602 nm ( $\epsilon = 108 \text{ M}^{-1} \text{ cm}^{-1}$ ) FT-IR (KBr pellet):  $\nu_{\text{ClO}_4^-}$ , 1110, 1090, 625  $\text{cm}^{-1}$ . X-band EPR data:  $g_{\text{av}}$ , 2.10. Molar conductance:  $\Lambda_{\text{M}}$  ( $\Omega^{-1} \text{ cm}^2 \text{ mol}^{-1}$ ), 235 in acetonitrile.  $\mu_{\text{eff}}$ : 1.62 BM.

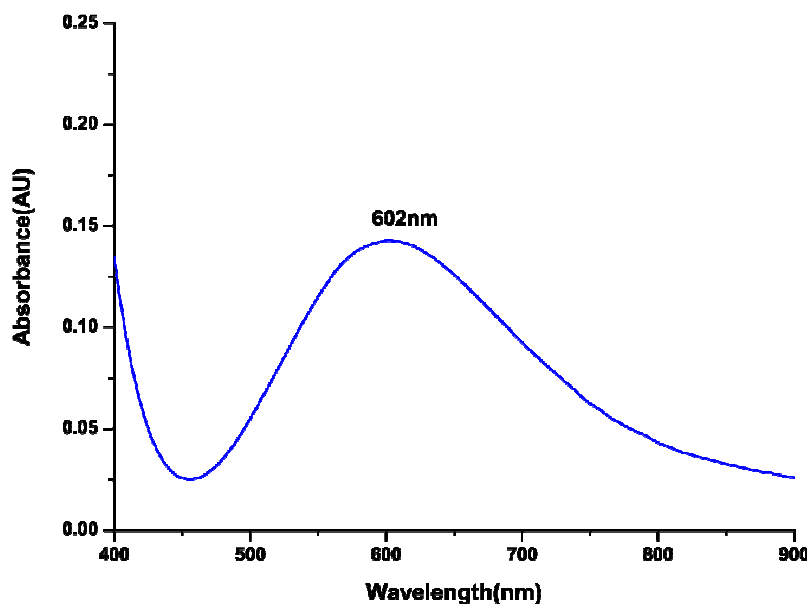


**Figure: S59:** UV-visible spectrum of Copper(II) complex of TMEDA ligand (**Complex 4**) in acetonitrile.

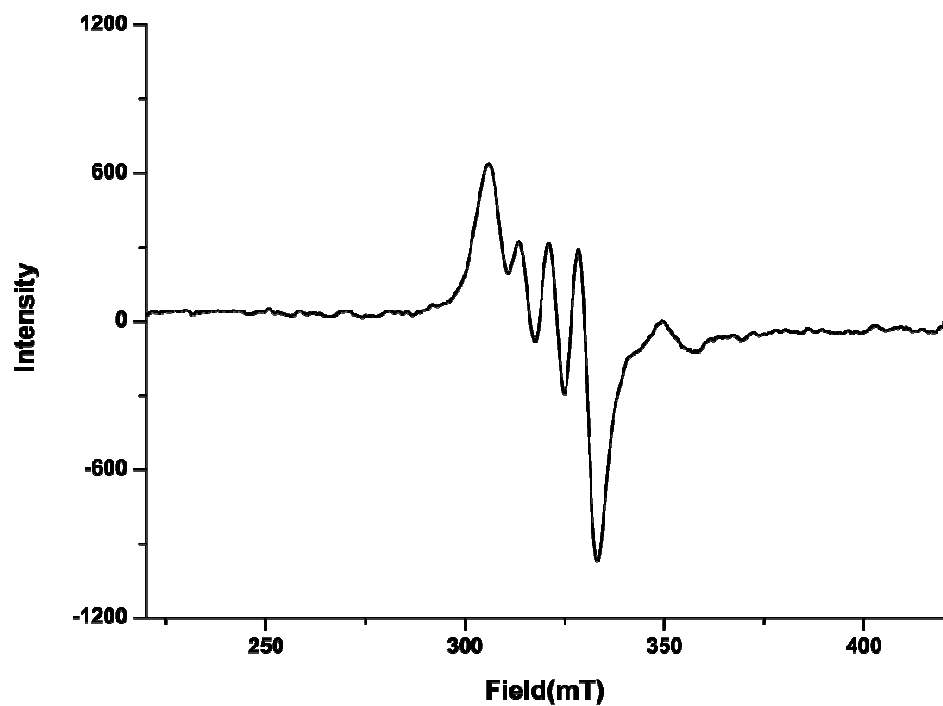


Figure S60: X-band EPR spectrum of complex **4** in acetonitrile at room temperature.

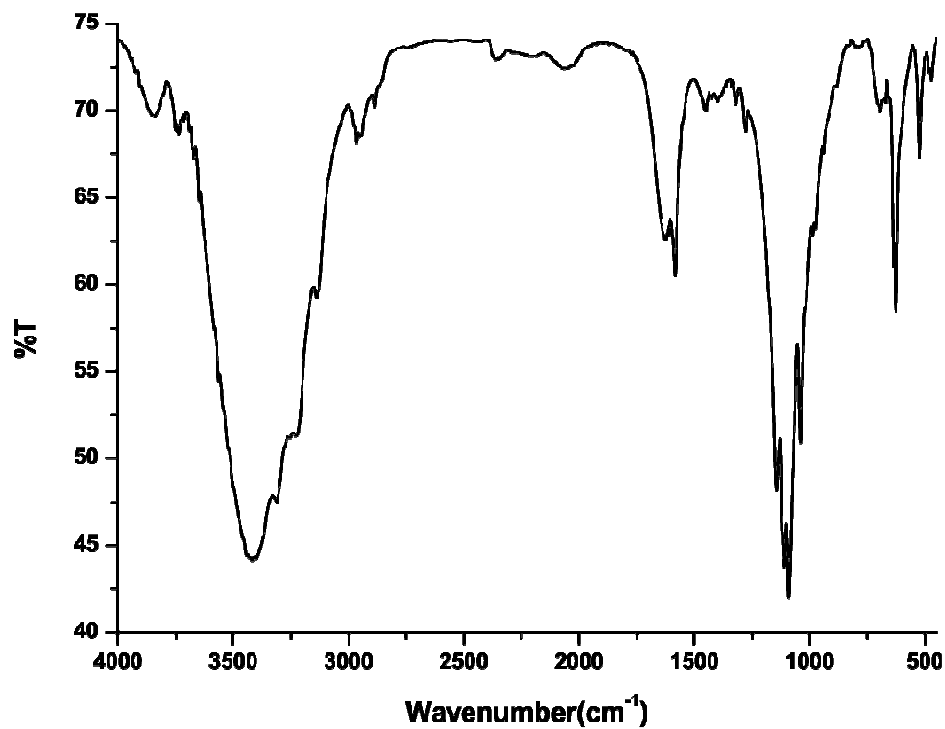
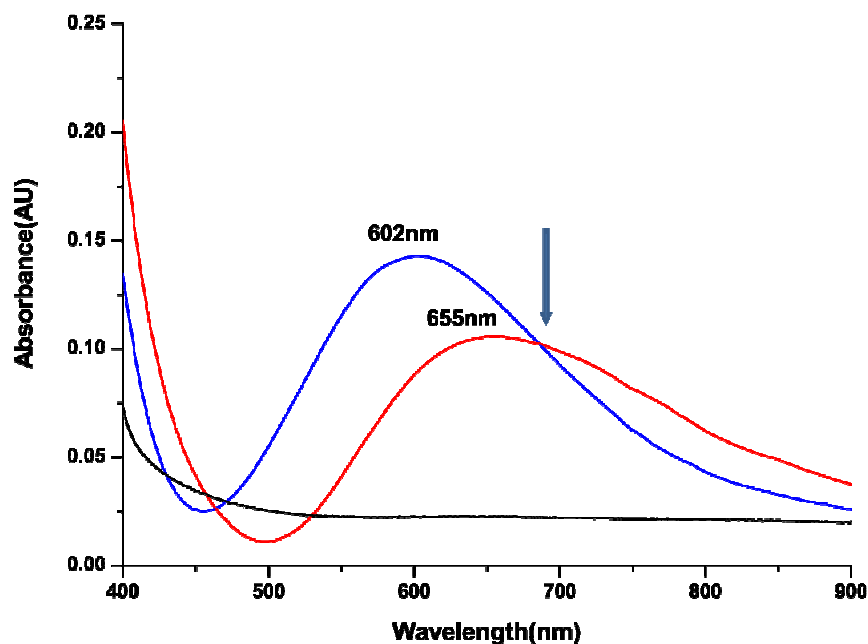
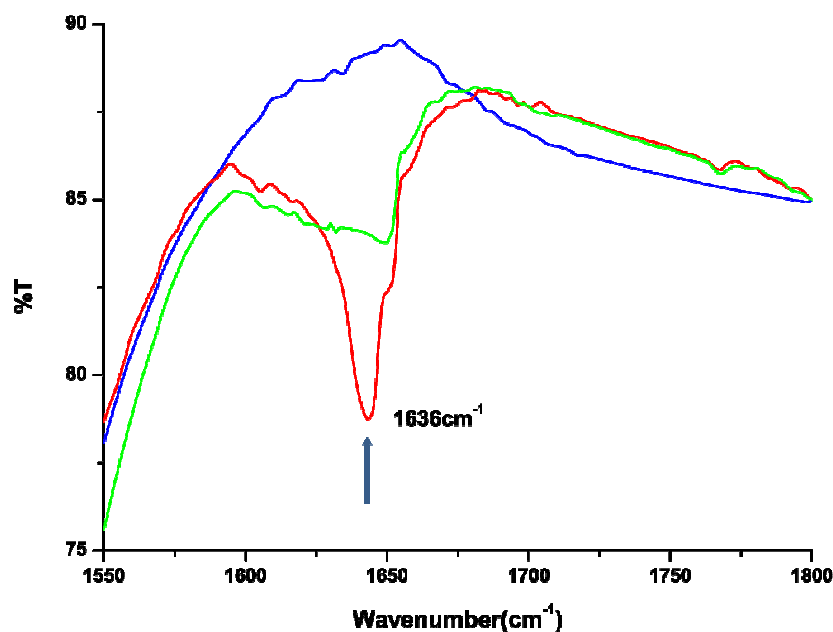


Figure S61: FT-IR spectrum of complex **4** in KBr.



**Figure S62:** UV-visible spectra of the reaction of complex **4** with nitric oxide in acetonitrile solvent at room temperature. (Blue trace represents the  $\text{Cu}^{\text{II}}$ -species, red represents that of the  $[\text{Cu}^{\text{II}}\text{-NO}]$  intermediate which gradually reduced to  $\text{Cu}^{\text{I}}$ -species (black).



**Figure S63:** Solution FT-IR spectra complex **4** in acetonitrile. (Blue trace represents solution FT-IR spectrum of complex **4**, red represents that immediately after purging nitric oxide and green represents that after 10 minutes.).

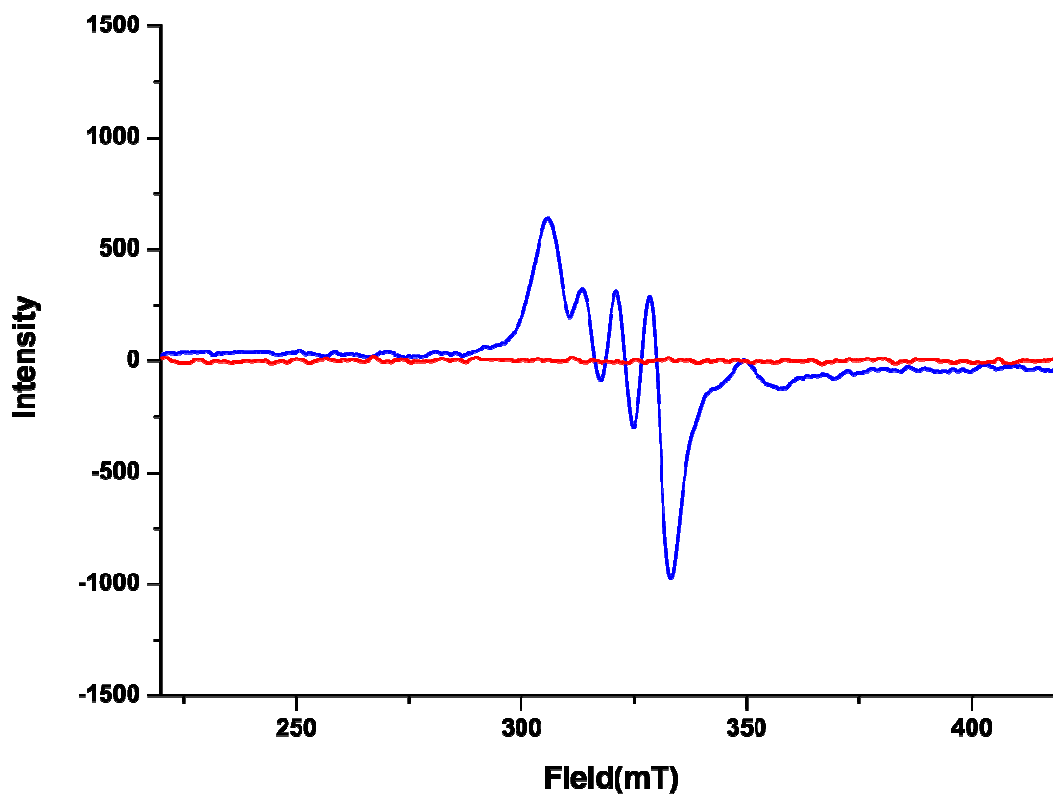


**Figure S64:** X-Band EPR spectra of complex **4** before (blue trace) and after (red trace) purging NO in acetonitrile at room temperature.

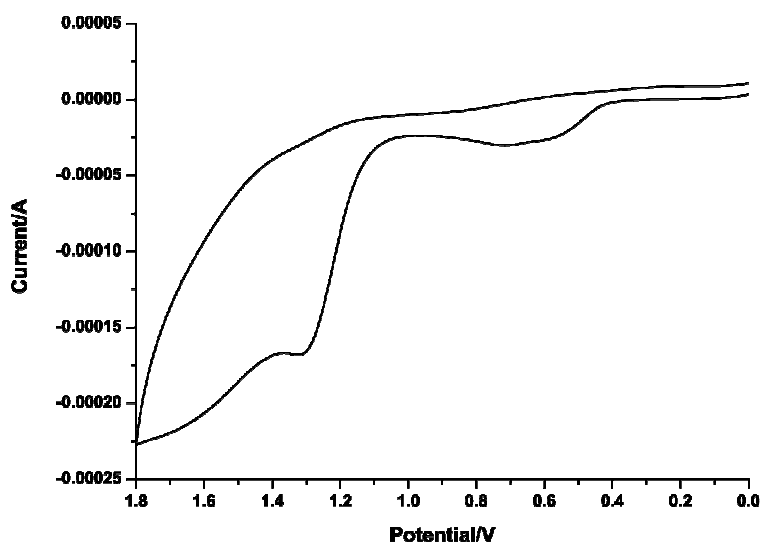


**Figure S65:** Cyclic voltammogram of complex **1** in acetonitrile solvent. (Tetrabutylammonium perchlorate supporting electrolyte; Pt working and SCE reference electrode and 50 mv/s scan rate).

**Reference:**

1. R. K. Harris; R. A. Spragg, *J. Mol. Spect.* 1969, **30**, 77.